Research in Pharmaceutical Sciences, June 2025; 20(3): 316-342
Received: 27-02-2025
Peer Reviewed: 15-03-2025
Revised: 14-04-2025
Accepted: 04-05-2025
Published: 17-06-2025

School of Pharmacy & Pharmaceutical Sciences
Isfahan University of Medical Sciences

Original Article

Synthesis and *in vitro* evaluation of novel pH-triggered biocompatible folate-chondroitin sulfate-dexamethasone copolymers for delivery of tofacitinib in rheumatoid arthritis

Zahra Ansarypour[1], Jaber Emami[1,*], Farshid Hassanzadeh[2], Mahmoud Aghaei[3], Mohsen Minaiyan[4], Neal M. Davies[5], and Mahboubeh Rezazadeh[1]

[1]*Department of Pharmaceutics, School of Pharmacy and Pharmaceutical Sciences, Isfahan, University of Medical Sciences, Isfahan, I.R. Iran.*
[2]*Department of Medicinal Chemistry, Faculty of Pharmacy and Pharmaceutical Science, Isfahan University of Medical Science, Isfahan, I.R. Iran.*
[3]*Department of Clinical Biochemistry, School of Pharmacy and Pharmaceutical Sciences, Isfahan University of Medical Sciences, Isfahan, I.R. Iran.*
[4]*Department of Pharmacology, School of Pharmacy and Pharmaceutical Sciences, Isfahan University of Medical Sciences, Isfahan, I.R. Iran.*
[5]*Faculty of Pharmacy and Pharmaceutical Sciences, Katz Centre for Pharmacy and Health Research, University of Alberta, Edmonton, AB, T6G 2E1, Canada.*

Abstract

Background and purpose: Rheumatoid arthritis (RA) is a chronic inflammatory disease associated with systemic complications and progressive disability. Systemic side effects and poor drug delivery to joints limit current treatments. This study aimed to enhance the efficacy of tofacitinib (Tofa) by synthesizing novel pH-triggered biocompatible polymers, both folate-targeted and non-folate-targeted.
Experimental approach: First-generation polymers were synthesized and characterized using FT-IR and ^{1}H-NMR spectroscopy. The critical micelle concentration of the copolymers was evaluated, and Tofa-loaded micelles were prepared using the dialysis method. The physical properties of the micelles were assessed using FE-SEM and dynamic light scattering. Cytotoxicity of Tofa/ chondroitin sulfate-maleic-dexamethasone (Tofa/CHS-Mal-DEX) and Tofa/folic acid-polyethylene glycol-chondroitin sulfate-maleic-dexamethasone (Tofa/FA-PEG-CHS-Mal-DEX) micelles was evaluated on the fibroblastic L929 and RAW264.7. The cellular uptake and anti-inflammatory effects were investigated in the activated Raw 264.7 cell line.
Findings/Results: Tofa/CHS-Mal-DEX and Tofa/FA-PEG-CHS-Mal-DEX micelles exhibited particle sizes of 188 nm and 173.06 nm, respectively, with entrapment efficiencies of 51% and 72.76%. The release profiles exhibited that about 40% of Tofa was released from micelles over 62 h in physiological pH, whereas in acidic conditions, this significantly decreased to 2 h. Micelles demonstrated improved uptake efficiency, resulting in a significant reduction in IL-6 levels compared to free Tofa. None of the micelle formulations indicated cytotoxic effects on fibroblastic L929 and Raw 264.7 macrophage cell lines.
Conclusion and implications: The developed folate and non-folate-targeted micelles were not toxic and biocompatible for enhancing the therapeutic potential of Tofa in RA and improving drug delivery.

Keywords: Chondroitin sulfate, Dexamethasone, Folic acid, Tofacitinib, pH-sensitive copolymers, Rheumatoid arthritis.

INTRODUCTION

Rheumatoid arthritis (RA) is a destructive inflammatory disease characterized by symmetric, peripheral polyarthritis, which results in functional disability, substantial pain, and joint deformity (1).

*Corresponding author: J. Emami
Tel: +98-3137927111, Fax: +98-3136680011
Email: Emami@pharm.mui.ac.ir

Access this article online

Website: http://rps.mui.ac.ir

DOI: 10.4103/RPS.RPS_40_25

RA patients are typically supported by treatment strategies including corticosteroids and non-steroidal anti-inflammatory drugs (NSAIDs) for controlling inflammation and pain; the disease-modifying anti-rheumatic drugs (DMARDs) for preventing joint damage; biological response modifiers that selectively inhibit special molecules involving five different modes of action such as tumor necrosis factor-alpha (TNF-α) inhibitors (infliximab, etanercept, adalimumab, certolizumab, golimumab), T cell co-stimulation blockade (abatacept), interleukin-6 (IL-6) receptor inhibitors (tocilizumab, tofacitinib (Tofa), baricitinib), B cell depletion (rituximab), and IL-1 inhibition (anakinra) of the immune system (2-4). Unfortunately, these drugs exhibit toxicity, short half-lives, and adverse extra-articular effects when used in large doses for long periods. Their non-selective distribution also remains a major clinical concern (5).

Tofa is a small-molecule inhibitor that modulates intracellular signaling pathways and primarily inhibits Janus kinase 1 (JAK1) and JAK3, which mediate signaling of the receptors for the common γ-chain-related cytokines IL-2, 4, 7, 9, 15, and 21, as well as interferon gamma and IL-6. The oral formulation of this drug is approved as an immediate-release tablet and may be administered at a dose of 5 mg twice daily for a total daily dose of 10 mg. While this dosage demonstrated significant clinical efficacy in alleviating RA symptoms compared to placebo (1,4), it also correlated with diminished patient compliance in the use of the drug and a higher incidence of adverse effects, specifically elevated serum transaminases indicative of liver injury, neutropenia, increased cholesterol levels, elevation in serum creatinine, and increased risk of infections. In human subjects, lymphopenia, neutropenia, and anemia are the Tofa side effects that lead to discontinuation of therapy if severe (6,7). The pharmacokinetic profile of Tofa is characterized by an elimination half-life of 3.2 h, with time to maximum plasma concentration (t_{max}) of 0.5 to 1 h. In RA, dexamethasone and Tofa work synergistically by dual suppression of lymphocyte proliferation and targeting separate arms of the immune response, glucocorticoid receptor pathways and JAK/STAT signaling, resulting in enhanced suppression of inflammation and the potential for lower and safer corticosteroid dosage (8,9). In collagen-induced arthritis rat models, Tofa alone had a modest effect, but dexamethasone significantly reduced inflammation. Their combination produced additive benefits, reducing paw swelling more effectively than either drug alone (9).

Establishing a drug delivery system based on joint targeting may be an attractive option accomplished by combining nanotechnologies of receptor-mediated active and passive targeting. Similar to the classic enhanced permeability and retention (EPR) effect observed in tumor tissues, colloid-based targeted drug delivery systems by a process of extravasation through leaky vasculature and subsequent inflammatory cell-mediated sequestration (ELVIS), connected with suitable ligand for particular receptor overexpressed on cells involved in the pathogenesis of RA can target drugs specifically to the region of inflammation (5,10-12) and promote efficient uptake of the particles into the diseased cells *via* a ligand-receptor mediated endocytosis (13). In RA, chronic inflammation causes the synovial blood vessels to become leaky due to cytokines like TNF-α and IL-1β, allowing nanoparticles to extravasate passively into the inflamed tissue. Once in the joint, these particles are actively taken up and retained by immune cells such as macrophages and neutrophils, which are abundant at the inflammation site. This process enhances local drug concentration and reduces systemic side effects. Unlike the EPR effect observed in tumors, where poor lymphatic drainage allows for passive accumulation of drugs, the ELVIS mechanism includes both vascular leakiness and active sequestration by inflammatory cells, making it particularly effective for inflammatory diseases such as RA (10-12). Polymeric micelles are exciting modern drug delivery systems that trap lipophilic drugs in their central hydrophobic domain, delivering their cargo to target tissues. Numerous studies on the evolution of polymeric micelles in targeted drug delivery systems have been conducted and site-specific drug delivery can be accomplished by

conjugating targeting agents. After arriving at the target area, these micelles release drugs by external stimulus, thereby enhancing the therapeutic efficacy and minimizing possible side effects (14-16). Synovial fibroblasts contain cells that have much higher CD44, a major pathogen that facilitates inflammation, cell migration, and activation of lymphocyte signaling receptors on their surface than other cells (17,18). One of the most important natural extracellular matrices, glycosaminoglycans, is hyaluronic acid, which connects to CD44 receptors and has been used in different investigations for targeted purposes. In addition, other amino glycans, involving heparan sulfate and chondroitin sulfate, can also attach to these receptors. Several studies demonstrate that some aminoglycans, such as chondroitin sulfate, can link to similar areas of the hyaluronic acid binding sites of CD44 receptors and compete with hyaluronic acid for binding to these receptors (19). Recently, Wang *et al.* developed self-assembled ROS-responsive nanoparticles of cholesterol-chondroitin sulfate by the inflammation-responsive di selenide bonds, and encapsulated Tofa and SP600125, as two kinase inhibitors, in aqueous media. This nano-drug delivery system can gather in inflammatory sites in arthritis areas and release its payloads for RA treatment (15). In addition to the CD44 receptor, folate receptor β, present on the surface of RA synovial macrophages, is another desirable candidate for active drug delivery in RA treatment because of its high binding affinity to folate (20). Moreover, the folic acid (FA) molecule has been widely used as a targeting agent in various drug carriers because of its small molecular size, less immunogenicity, high stability, and inexpensive cost (21).

The acidic pH of the microenvironment of joint inflammation and endolysosomes (pH about 4.5-5.5) creates an ideal opportunity to employ pH-sensitive drug delivery systems, which can respond to the local pH changes by releasing their therapeutic cargo specifically at the site of inflammation (22). Because of the two adjacent carboxylic groups in each monomer unit, maleic acid copolymers are classified as weak anionic polyelectrolytes and undergo a two-step dissociation process. First dissociation: maleic acid (H_2MA) loses one proton to form a mono-protonated species (HMA^-). Second dissociation: the mono-protonated species (HMA^-) loses another proton to form the fully deprotonated maleate ion (MA^{2-}). At low pH, the high concentration of H^+ ions favors the protonation of the maleate ions, shifting the equilibrium towards the undissociated maleic acid form (H_2MA). At high pH, the lower concentration of H^+ ions favors the dissociation of maleic acid, leading to the formation of more maleate ions (MA^{2-}). These dissociation processes result in an enlarged pH-sensitivity window, allowing them to respond distinctly to changes in pH, which makes them useful in pH-sensitive controlled drug release systems (23,24). To the best of our knowledge, the polymeric micelles with targeting agents of chondroitin sulfate and FA for RA drug delivery have not been reported. Due to the pH-sensitive characteristic of maleic anhydrides (25), and because of the therapeutic and targeting potential of chondroitin sulfate in targeting synovial tissue cells, in the present study, a pH-sensitive chondroitin sulfate-maleic-dexamethasone copolymer was first synthesized and subsequently used for targeting the inflammatory tissue, the chondroitin sulfate copolymer was conjugated with polyethylene glycol (PEG). Thus, we focused on the synthesis and some of the physical properties of chondroitin sulfate-maleic-dexamethasone (CHS-Mal-DEX) and FA-PEG-CHS-Mal-DEX micelles containing Tofa separately or in combination. The *in vitro* cell culture studies were also investigated in detail.

MATERIALS AND METHODS

Materials

Chondroitin sulfate sodium (CHS; MW: 10 kDa) from Biotech Company (India), , Tofa citrate from Nano Alvand Company (Iran), DEX from Iran Hormone Company (Iran), FA, dicyclohexyl carbodiimide (DCC), N-hydroxy succinimide (NHS), maleic anhydride (Mal), polyethylene glycol-di-amine (MW: 3 kDa), and dialysis bag (molecular weight cutoff, MWCO: 2 kDa, 8-10 kDa and 10-12 kDa) from Sigma-Aldrich Company (Germany). Anhydrous dimethyl sulfoxide

(DMSO), formamide and dimethylformamide (DMF) from Samchun Company (South Korea), acetone, sodium hydroxide, and methanol from Merck Company (Germany). Trypsin, fetal bovine serum (FBS), and Dulbecco's modified eagle medium (DMEM) high glucose from BIO-IDEA (USA, New York), KPG-MIL-6 ELISA kit for measuring mouse IL-6 from Karmania Pars Gene (Iran).

Synthesis of CHS-Mal-DEX copolymer

The two-step esterification reactions accomplished the synthesis of CHS-Mal-DEX conjugate. Firstly, the Mal-DEX was synthesized by an esterification process previously reported (26). Briefly, DEX (0.25 mmol, 100 mg) was dissolved in 10 mL glacial acetic acid in a dried one-neck flask, and Mal (0.5 mmol, 30 mg) was added to the flask. Then, three drops of sulfuric acid were mixed to catalyze the esterification reaction and stirred at room temperature for 24 h. The mixture was then added to 25 g of ice to stop the reaction and precipitate Mal-DEX. Then, the resulting precipitate was centrifuged at 13,000 rpm for 15 min and dried with nitrogen gas. Subsequently, CHS was linked with Mal-DEX by the esterification reaction between the hydroxyl group of CHS and the carboxyl group of Mal-DEX (27). The Mal-DEX (0.017 mmol, 8.6 mg), DCC (0.051 mmol, 10.52 mg), and 4-dimethylaminopyridine (0.034 mmol, 4.153 mg) were dissolved in 3 mL anhydrous DMF and stirred for 24 h under the protection of nitrogen to activate the COOH group of Mal-DEX. Then, different amounts of CHS, dissolved in 5 mL of formamide with gentle heating, were inserted into the reaction mixture and continued for 48 h under a nitrogen atmosphere. The mixture was added into a 3-fold volume of acetone and the final precipitate was centrifuged. To separate unreacted material, the precipitate was added to dialysis membranes (MWCO: 8-10 kDa) and dialyzed against methanol and phosphate buffer (0.001 mM, pH 7.4) for 24 h and 48 h, respectively. Then, the resulting product was lyophilized by a freeze dryer (Model ALPHA 2-4 LD plus, Christ Company, Stuttgart, Germany) to obtain the CHS-Mal-DEX pure powder.

Synthesis of FA-PEG

Briefly, FA (88.3 mg, 0.2 mmol), DCC (123.6 mg, 0.6 mmol), and NHS (69.3 mg, 0.6 mmol) were dissolved in anhydrous DMSO under nitrogen protection in a dried 3-neck flask and stirred for 24 h in the dark condition at room temperature to activate the COOH group of FA. After that, PEG-di-amine (300 mg, 0.1 mmol) in DMSO was poured into the activated folate solution and the reaction mixture was stirred for 24 h under the same conditions. Finally, the mixture was dialyzed (MWCO: 2 kDa) against methanol and deionized water for 24 h and lyophilized to acquire the FA-PEG pure yellow powder (28,29).

Synthesis of FA-PEG-CHS-Mal-DEX

The CHS-Mal-DEX co-polymer was attached to the FA-PEG by the amidation reaction between the free amine group of FA-PEG and the COOH group of CHS. Briefly, FA-PEG (0.015 mmol, 7 mg) was dissolved in anhydrous DMSO and CHS-Mal-DEX was dissolved in the mixture of formamide and anhydrous DMSO with gentle heating and then mixed with the FA-PEG solution and stirred for 8 h under nitrogen gas. After that, DCC and NHS were added to the solution and the reaction was resumed for 72 h at room temperature. The mixture was then diluted by a 3-fold volume of phosphate buffer (0.001 mM, pH 7.4), and afterwards dialyzed (MWCO: 10-12 kDa) against methanol followed by phosphate buffer (0.001 mM, pH 7.4) for 24 h and consequently, was lyophilized to achieve a pale-yellow powder (28,29).

FA-PEG-CHS-Mal-DEX copolymer characterization

Synthesis of the final targeted copolymer (FA-PEG-CHS-Mal-DEX), non-folate-targeted copolymer (CHS-Mal-DEX), FA-PEG, and Mal-DEX was confirmed by Fourier transform infrared (FT-IR; (Rayleigh, WQF-510/520, China, 400-4,000 cm^{-1}) and ^{1}H-nuclear magnetic resonance (^{1}H-NMR; (Bruker Biospin, 400MHz, Germany). For the FT-IR evaluation, a suitable quantity of the lyophilized powder and KBr was ground and turned into a compressed disk. For ^{1}H-NMR

examination, each targeted and non-folate-targeted copolymer was dissolved in the appropriate mixture of DMSO-d_6: D_2O (1:4), and FA-PEG was dissolved in DMSO-d6 (28,29).

Determination of critical micelle concentration

Pyrene as a hydrophobic fluorescence probe was used to determine the critical micelle concentration (CMC) of CHS-Mal-DEX and FA-PEG-CHS-Mal-DEX by the fluorescence spectroscopy method (28,30,31). Briefly, 5×10^{-6} mol/L of pyrene solution in acetone was added to glass tubes and then the solvent was evaporated by a stream of nitrogen gas. Afterward, polymer solutions with various concentrations (0.025 to 1000 µg/mL) were added to each tube to obtain the final pyrene concentration of 5×10^{-7} mol/L. The mixture was shaken for 48 h at 37 °C in the dark. Then, the pyrene's fluorescence emission spectra in different polymer solutions were screened by a spectrofluorometer (Jasco FP 750, Tokyo, Japan) at the excitation wavelength of 336 nm. The intensity ratio of the first peak (I_1, 375 nm for CHS-Mal-DEX and I_1, 370 nm for FA-PEG-CHS-Mal-DEX) to the third peak (I_3, 387 nm for CHS-Mal-DEX and I_3, 380 nm for FA-PEG-CHS-Mal-DEX) was drawn against the logarithm of polymer concentration, from the pyrene emission spectra. Finally, two tangents were plotted and the CMC value was taken from the intersection.

Preparation of free drug base

To prepare the drug-free base, 4 mg of Tofa citrate was dissolved in 8 mL of deionized water. Then, ethylene diamine at different molar ratios (1, 3, 6, and 9) was added, and each solution was stirred for 24 h under dark conditions at room temperature to eliminate citrate, and the free base of Tofa was precipitated. Finally, the precipitant was washed twice with deionized water and white powder was collected (32,33).

Preparation of polymeric micelles

Tofa was incorporated into polymeric micelles using either the probe-type ultrasonication technique or the dialysis method.

Probe-type ultrasonication technique

A probe-type ultrasonication technique was used to prepare Tofa-loaded polymeric micelles. CHS-Mal-DEX and FA-PEG-CHS-Mal-DEX (10 mg) were dispersed in distilled water and stirred for 2 h at room temperature. Tofa (1 and 2 mg) was dissolved in anhydrous methanol, and then the Tofa solution was injected dropwise into the polymer solution with stirring at different rpm (300 and 600) at room temperature. The mixture was ultrasonicated (2 and 3 s on and off, respectively) for 2.5, 5, and 7.5 min with an output power of 40 W (JY 92-II Ultrasonic Processor, Shanghai, China) in an ice bath after stirring at room temperature for 24 h. The resultant Tofa-loaded micellar solution was centrifuged at 3500 rpm for 10 min and the supernatant was collected (34).

Dialysis method

Ten mg of each copolymer (CHS-Mal-DEX and FA-PEG-CHS-Mal-DEX) was dissolved in 9 mL of DMSO: H_2O (2:1) and Tofa (2 mg) pre-dissolved in 1 mL of DMSO was injected dropwise and stirred for 6 h; then 6 mL of deionized water was added and stirred for 14 h. The solution was loaded into a dialysis bag (MWCO: 8-10 kDa) obtained from Spectrum Labs, Inc., Houston, TX, and dialyzed against deionized water (500 mL, 4 h). The solution of micelles was collected and frozen at -80 °C for 2 days and lyophilized to obtain dried micelles (35).

Characterization of Tofa-loaded polymeric micelles

Morphological evaluation of polymeric micelles by scanning electron microscope and Transmission electron microscope

The optimized formulation was coated with gold and surface morphology was observed under a field emission scanning electron microscope (FE-SEM; QUANTA FEG 450, FEITM, USA) at 15 kV. Polymeric samples were adsorbed on the carbon-coated grid. For transmission electron microscope (TEM) observation, a drop of sample solution was

placed onto a carbon-coated copper grid and dried for 15 min in air. Finally, TEM (EM10C, Germany), operated at a voltage of 80 kV, was used for observation.

Determination of zeta-potential and particle size

The polymeric micelles' particle size, Zeta potential, and polydispersity index (PDI) in aqueous media were determined by dynamic light scattering (DLS) utilizing Malvern Zeta-sizer Nano-ZS (Malvern Instruments Ltd., UK) at room temperature.

Determination of encapsulation and loading efficiencies

Tofa-containing micellar solution (200 µL) was diluted with 9.8 mL of methanol and treated with ultrasonics in a water bath at room temperature for 20 min. Afterward, the Tofa content was determined by UV spectrophotometry at a detection wavelength of 287 nm. Finally, the percentage of entrapment efficiency (EE) and loading efficiency (LE) were calculated using the following equations:

$$\text{EE (\%)} = \frac{\text{Weight of the drug in the micelles}}{\text{Weight of the feeding drug}} \times 100 \quad (1)$$

$$\text{LE (\%)} = \frac{\text{Weight of the drug in the micelles}}{\text{Weight of the micelles}} \times 100 \quad (2)$$

In vitro release of Tofa from polymeric micelles

The release of Tofa from polymeric micelles in PBS (0.01 M) with different pHs (5 and 7.4) at 37 ℃ was determined *in vitro*. The lyophilized micelle powder loaded with Tofa in various weight ratios to the copolymer was dissolved in PBS 0.01 M, pH 7.4. The resulting solution was placed in a dialysis bag (MWCO: 10-12 kDa), and the bag was immersed in a glass beaker with a 30 mL release medium with agitation of 100 rpm at 37 ℃. At predetermined time intervals, samples were withdrawn and replaced with fresh medium maintained at the same temperature. The content of Tofa in the samples was determined by the UV spectroscopy method at a detection wavelength of 287 nm.

Micellar stability study

Tofa-loaded polymeric micelles with a drug/polymer (D/P) ratio of 5, prepared by the dialysis method, were used to perform stability studies. The particle size of Tofa-loaded micelles in PBS containing 10% FBS was recorded by the DLS method over 48 h and defined as t_i. The average diameter of micelles in PBS before FBS treatment, t_0, was also measured. The ratio of particle sizes was calculated as t_i/t_0. For long-term stability, the lyophilized powder of Tofa-loaded micelles was stored in a refrigerator at 4 ℃ for two months. Then, the changes in particle size, Zeta potential, and drug content during the storage were measured (28,29).

In vitro cell culture studies

The RAW264.7 and L929 cell lines were grown in 25-cm³ flasks and incubated in 5% CO_2, 95% humidity, and 37 °C, in high-glucose DMEM medium, supplemented with 10% FBS, 100 U/mL penicillin, and 100 µg/mL streptomycin.

Evaluation of L929 and RAW 264.7 cells' viability

The viability of fibroblastic L929 cells and RAW 264.7 cells exposed to different formulations was evaluated by MTT assay. For this purpose, the L929 and RAW 264.7 cells were poured into 96-well plates with a population of 5×10^3 and 8×10^3 cells per well, respectively. After incubation for 24 h at 37 °C, cells were treated with different formulations containing free drug (0, 0.5, 1, 2.5, 5, and 10 µg/mL), CHS-Mal-DEX micelles containing Tofa (0, 0.5, 1, 2.5, 5, and 10 µg/mL), and FA-PEG-CHS-Mal-DEX micelles containing Tofa (0, 0.5, 1, 2.5, 5, and 10 µg/mL). Then, 20 µL of MTT solution (5 mg/mL in PBS) was added to each well, followed by incubation for another 3 h. Next, the culture medium was decanted, and 150 µL of DMSO was added to dissolve the precipitates and the absorbance was detected by a Thermo MK3 ELISA reader at 570 nm. The assays were conducted in 3 replicates for each independent test. The statistical mean and standard deviation were used to represent the cell viability.

Cellular uptake study

To test the intracellular delivery of molecules by micelles developed in this study, lipophilic coumarin (CMN), which shows

green fluorescence, is loaded into CHS-Mal-DEX and FA-PEG-CHS-Mal-DEX micelles. Cellular internalization of CMN was studied using fluorescence microscopy and flow cytometry on RAW 264.7 cells. Briefly, RAW 264.7 cells were seeded in 12-well plates with a cell density of 1×10^5 per well. The cells were stimulated by lipopolysaccharide (LPS) for 24 h. Next, the medium was exchanged for fresh medium and the cells were treated with CMN solution, CMN-loaded CHS-Mal-DEX, and CMN-loaded FA-PEG-CHS-Mal-DEX for 4 and 6 h. The medium in each well was emptied and cells were washed with PBS (pH 7.4, 10 mM) and analyzed using fluorescent microscopy (16,36).

To quantify the cellular uptake, CMN solution, CMN-loaded CHS-Mal-DEX, and CMN-loaded FA-PEG-CHS-Mal-DEX were added to RAW 264.7 cells at a density of 2×10^5 cells per well of 6-well plates and cultured for 6 h, respectively. Subsequently, the medium was discarded, and cells were washed thrice using cold PBS. Five hundred µL of trypsin was added to each well and incubated for 5 min. Then, each well was neutralized with 1 mL complete culture medium, centrifuged at 1000 rpm/min for 5 min. The cell pellet was resuspended in 300 µL of PBS and analyzed using a BD FACS Canto II flow cytometer (BD Biosciences, Oxford, UK) (16,36).

In vitro anti-inflammatory assay in activated macrophages RAW264.7

For this purpose, RAW 264.7 cells with a density of 5×10^5 cells per well were seeded into 6-well plates. Then, cells were stimulated by 1 µg/mL of LPS for 4 h to establish inflammatory cell models. After 4 h, the culture media of wells were removed and treated with the culture media containing free drug (0.8 µg/mL), Tofa/CHS-Mal-DEX (0.8 µg/mL), and Tofa/FA-PEG-CHS-Mal-DEX micelles (0.8 µg/mL), respectively, for 24 h. Finally, to determine the concentration of IL-6, the cell supernatants were collected and tested by an ELISA kit (KPG-MIL-6) following the manufacturer's instructions. The LPS-treated and untreated RAW264.7 cells were tested as the positive (LPS^+) and negative (LPS^-) control groups, respectively (15,16).

Folate competitive inhibition assay

For the competition cell study, after 4 h of cells stimulated by LPS, the culture media of wells were removed and treated with the culture media containing 40 µg/mL of FA. After 12 h, Tofa/FA-PEG-CHS-Mal-DEX micelles (0.8 µg/mL) were added and incubated for 24 h. Finally, the cell supernatants were collected and assayed with an IL-6 ELISA kit (KPG-MIL-6).

A flow cytometry method assay was used to investigate folate competitive inhibition evaluation. After 12 h of cell incubation in FA-containing media, the CMN-loaded FA-PEG-CHS-Mal-DEX, CMN-loaded CHS-Mal-DEX, and free CMN were added and incubated for 6 h. Subsequently, the amount of CMN in cells was analyzed by a flow cytometer (BD Biosciences, Oxford, UK) (34).

Statistical analysis

Data are presented as mean ± SD of three separate experiments and are compared by an independent sample t-test for two groups, and one-way ANOVA followed by Tukey post-hoc test for more than two groups. *P*-values less than 0.05 were considered statistically significant in all cases.

RESULTS

Synthesis and characterization of CHS-Mal-DEX and FA-PEG-CHS-Mal-DEX copolymers

In the current study, an amphiphilic CHS-Mal-DEX copolymer was initially synthesized using Mal as a pH-sensitive spacer between DEX and CHS via two-step esterification reactions, as represented in Fig. 1A. Mal-DEX was synthesized by the reaction between the hydroxyl group of DEX and maleic anhydride. Next, the COOH group of Mal-DEX was activated and then connected to the free hydroxyl groups of the CHS backbone. To synthesize the FA-PEG-CHS-Mal-DEX conjugate, the FA molecule was first activated by DCC/NHS and then linked to the diamine-PEG via the amide linker. Then, the COOH group of CHS-Mal-DEX was linked to the free NH2 of FA-PEG conjugate by the amidation reaction. Figure 1B and C illustrate the synthetic scheme of these reactions.

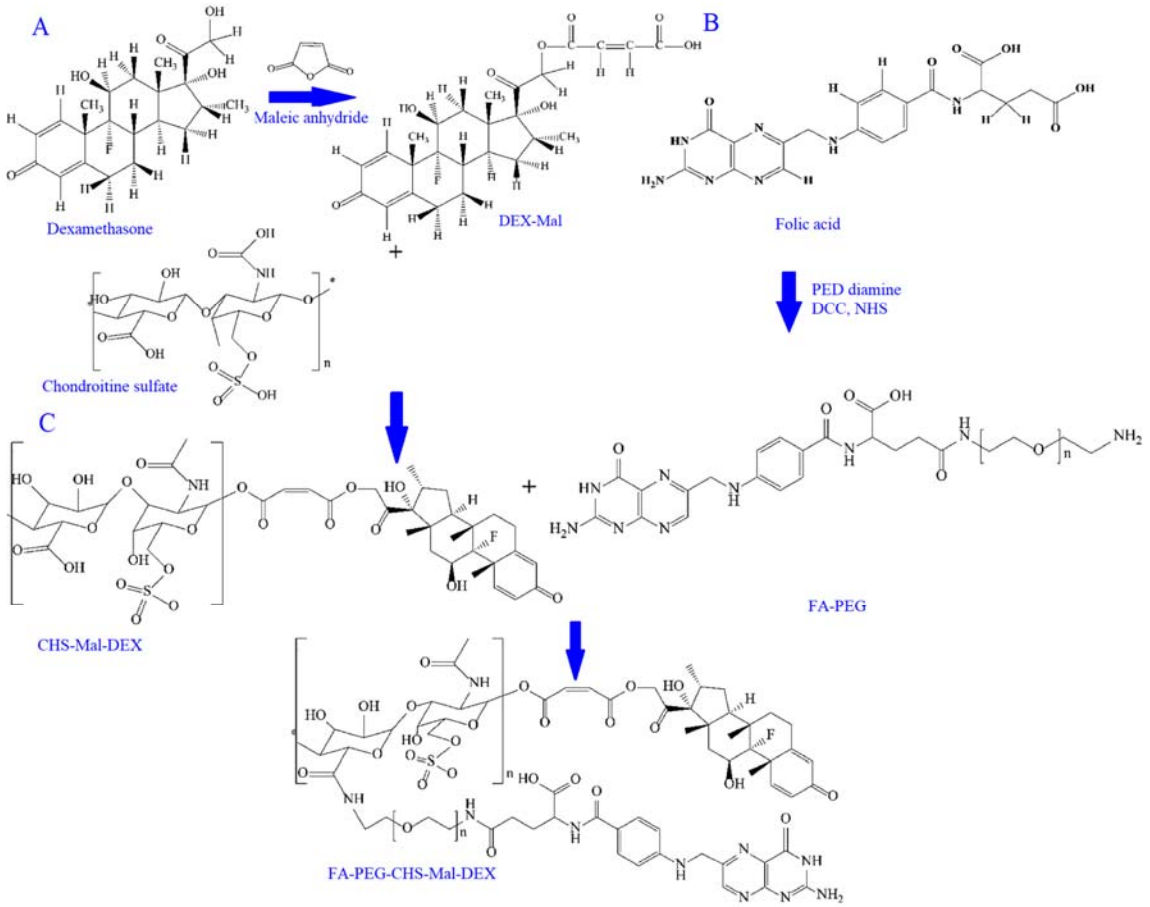

Fig. 1. Schematic presentation of FA-PEG-CHS-Mal-DEX conjugate synthesis. FA, folic acid; PEG, polyethylene glycol; CHS, chondroitin sulfate; Mal, maleic; DEX, dexamethasone; DCC, dicyclohexyl carbodiimide; NHS, N-hydroxy succinimide.

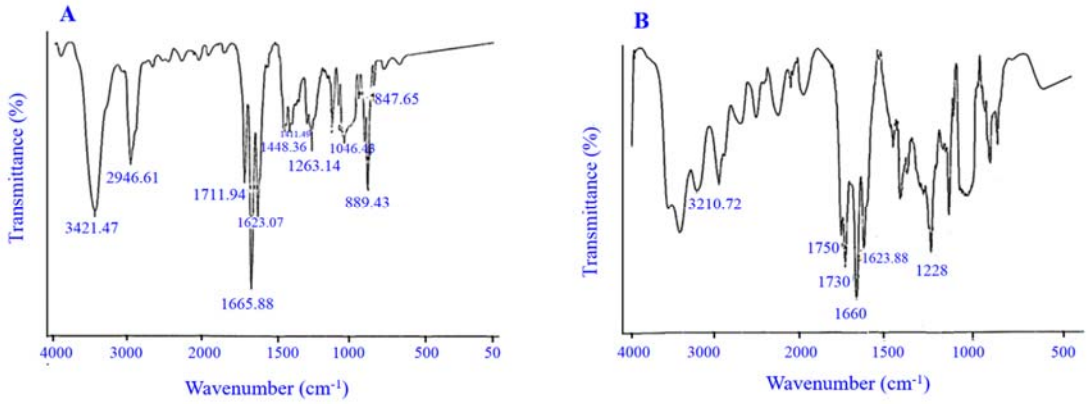

Fig. 2. FT-IR spectra of (A) dexamethasone and (B) dexamethasone-maleic.

Figures 2 to 9 illustrate the copolymer structures confirmed by FT-IR and 1H-NMR. Figure 2B depicts the FT-IR spectrum of DEX-Mal with characteristic bands of hydroxyl (OH) group of the carboxyl acid (COOH) at 3210.72 cm-1, carbonyl (C=O) of carboxyl (COOH) group at 1730 cm-1, carbonyl (C=O) of the steric bond at 1750 cm-1, the C=C stretching peak at 1660 and ether (C-O-C) stretching vibration at 1228 while not presented for DEX in Fig. 2A (27,37-39).

The FT-IR spectra of CHS and CHS-Mal-DEX (Fig. 3A and B) showed absorption bands at 850, 1261.26, and 1648.71 cm-1 corresponding to C-O-S, S-O, and C-O stretching vibration of the C=O group in acetylated amine (38,40,41). The intensity of the OH stretching band of CHS at 3592.89 cm-1 decreased after conjugation of Mal-DEX with CHS in the CHS-Mal-DEX spectrum (Fig. 3B). The C=O of the new steric linkage appeared at 1729.99 cm^{-1}. Two strong bands at 1250.01 and 1063 cm^{-1} indicate newly formed C-O of phenyl alkyl ethers is also evident. Additionally, the specific symmetric and asymmetric stretching vibration bands CH2 and CH3 of the DEX alkyl chain at 2923.88 and 3161 cm^{-1} were seen in the spectrum of CHS-Mal-DEX (38,40).

The FT-IR spectrum of PEG and FA-PEG (Fig. 4) exhibited a band at 1597 cm^{-1} corresponding to phenyl C=C stretching, which was also observed in the spectrum of FA-PEG (Fig. 4B). The band at 1110 cm^{-1} in the PEG (Fig. 4A) and FA-PEG spectra (Fig. 4B) is related to the C-O stretching of PEG. Furthermore, the band at 1683.66 cm^{-1} in the spectrum of FA-PEG (Fig. 4B), which is related to the C=O stretching vibration of the new amide bond, confirmed the formation of the FA-PEG molecule. Figure 5 shows the IR spectrum of FA-PEG-CHS-Mal-DEX, where two characteristic bands at 1657 and 1789.88 cm^{-1} are related to the formation of the new amide bond in the CHS backbone and steric bond of Mal-DEX conjugation, respectively (28,29,38).

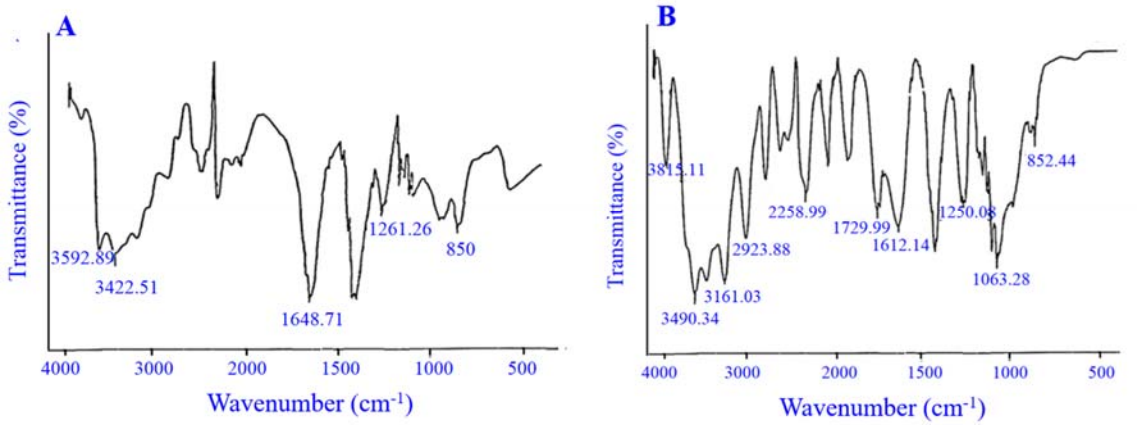

Fig. 3. FT-IR spectra of (A) CHS and (B) CHS-Mal-DEX. CHS, Chondroitin sulfate; Mal, maleic; DEX, dexamethasone.

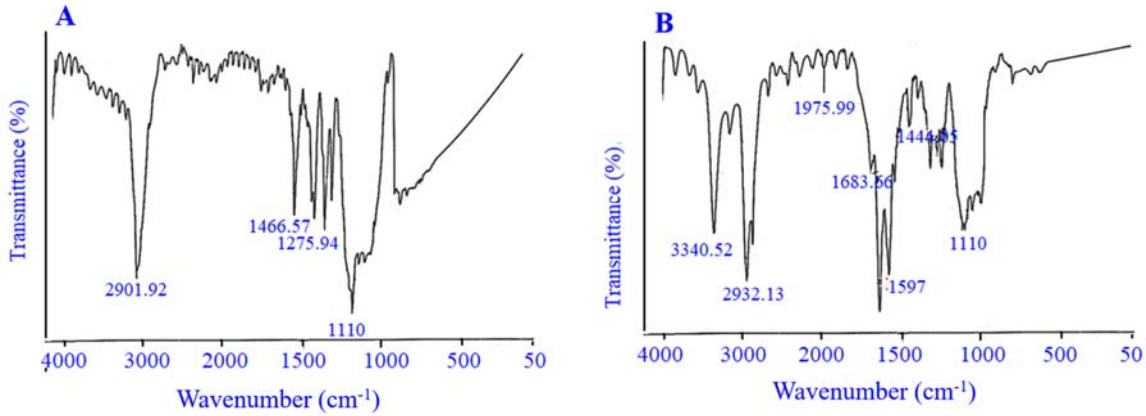

Fig. 4. FT-IR spectra of (A) PEG diamine and (B) FA-PEG. PEG, Polyethylene glycol; FA, folic acid.

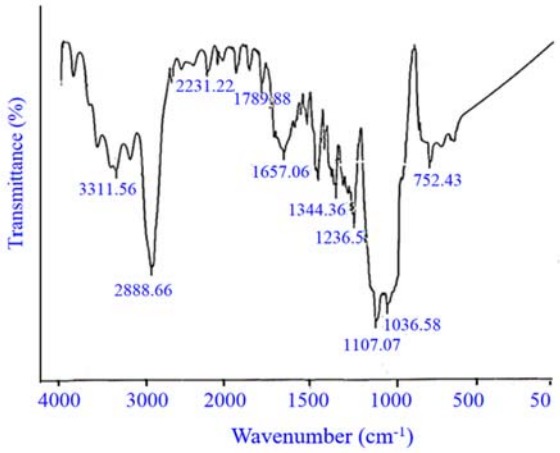

Fig. 5. FT-IR spectra of FA-PEG-CHS-Mal-DEX. FA, Folic acid; PEG, polyethylene glycol; CHS, chondroitin sulfate; Mal, maleic; DEX, dexamethasone.

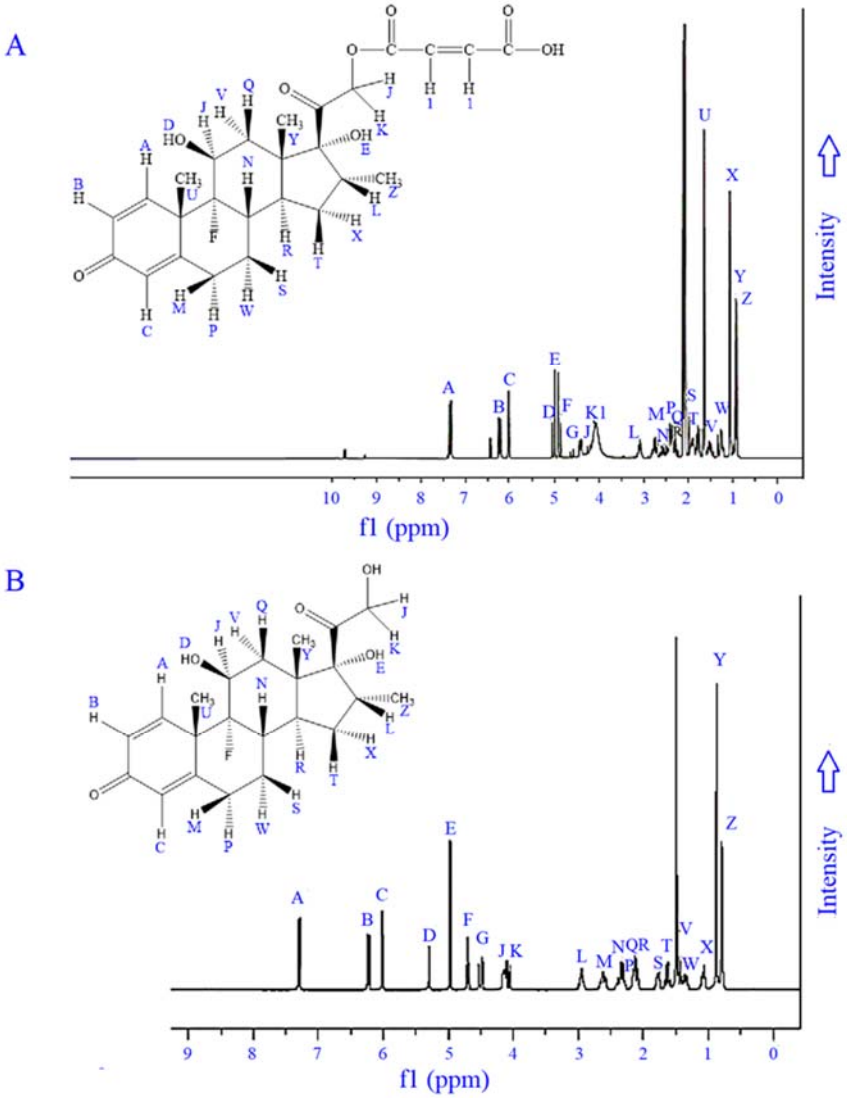

Fig. 6. [1]HNMR spectra of (A) Mal-DEX and (B) DEX. Mal, Maleic; DEX, dexamethasone.

The 1H-NMR spectrum of DEX-Mal (Fig. 6A) peaked at 3.8 ppm, corresponding to HC=CHCOOH groups of the Mal (42). The hydrogen peaks of the ring A of DEX (Fig. 6B) appeared at 7.29, 6.23, and 6.01 ppm in the spectra designated by A, B, and C, respectively. The peaks at 1.49, 0.88, and 0.78 ppm assigned by the letters U, Y, and Z, respectively, are attributed to the hydrogens of the CH3 groups of DEX. The peaks exhibited by the letters E, F, and D are related to the hydrogen of the OH groups of the rings C and D of DEX, respectively. These signals of the DEX spectrum were not observed at the same chemical shifts in the spectrum of CHS (Fig. 7A) and also appeared in the spectrum of DEX-Mal-CHS (Fig. 7B and C) (37,38,43).

In the spectrum of CHS (Fig. 7A), acetamide methyl protons around 2 ppm appeared in the upfield parts of the spectra, and the polysaccharide H-1(anomeric) protons at 4.0 - 5.0 ppm appeared in the downfield parts of the spectra. The peaks at around 4.2 and 4.7 ppm relate to H-4 signals of GalNAc residue, and the peaks at around 3.9, 4.1, and 4.5 ppm belong to H-5, H-2, and H-1 signals of GalNAc residue, respectively. The peaks at around 3.3, 3.5, 3.6, 3.7, and 4.4 are attributed to the H-2, H-3, H-5, H-4, and H-1 signals of GluUA residue, respectively (44). All CHS signals were also observed in the spectrum of DEX-Mal-CHS (Fig. 7B and C). All these findings confirm the successful conjugation of Mal-DEX onto the CHS backbone. The degree of substitution (DS) of CHS-Mal-DEX was measured by the peak areas of X, Y, and Z groups of the Mal-DEX (chemical shift from 0.78 to 1.06 ppm) and the acetamido methyl group of CHS (chemical shift from 1.8 to 2 ppm) using the equation (3) provided below (27,37):

$$\mathrm{DS}\ (\%) = \frac{\text{The integral of peaks from 0.78 to 1.06} \times 63}{\text{The integral of peaks from 1.8 to 2} \times 2 \times 21} \times 100 \quad (3)$$

For 10 and 20 feed molar ratios of Mal-DEX to CHS, DS was determined to be around 13.28 and 26.14 %, respectively.

The ^{1}H-NMR spectra of FA, FA-PEG, DEX-Mal-CHS, and FA-PEG-CHS-Mal-DEX are respectively shown in Figures 8A, 8 B, 7B, and 9. In Fig. 8A, the ^{1}H-NMR spectrum of FA peaks at 1.9, 2.2, and 4.3 ppm are assigned to the aliphatic protons of FA and peaks at 6.6, 7.6, and 8.6 ppm are attributed to the aromatic protons (28,29,45,46). These signals were also observed in the FA-PEG (Fig. 8B) and FA-PEG-CHS-Mal-DEX (Fig. 9) spectra. In the FA-PEG spectrum, -CH2- protons of PEG contributed to the chemical shift at 3.4 ppm, and the protons next to the amine group of the PEG were observed around 1.7 ppm (29,45). In the spectrum of FA-PEG-CHS-Mal-DEX, peaks around 2 ppm correspond to the acetamide methyl protons of CHS. The chemical shifts at 0.88 and 0.78 related to the hydrogens of methyl groups of DEX and the peak at 1.06 is contributed to the hydrogen of the D ring of DEX assigned by the letter X. The signal at 3.4 ppm contributed to -CH2- protons of PEG, and the peak at 8.6, 8.17, and 7.7 related to aromatic protons of FA. The peaks from 3.3 to 4.5 ppm correspond to sugar ring protons. All the findings confirm the successful conjugation of FA-PEG onto CHS-Mal-DEX.

Determination of CMC

The CMC was determined by measuring the intensity ratio (I_3/I_1) of the third peak, the highest energy bands in the emission spectra of pyrene and the first peak (28-30). Figure 10 shows the change in the value of (I_3/I_1) versus the logarithm of CHS-Mal-DEX or FA-PEG-CHS-Mal-DEX concentrations. As indicated in Fig. 10, by increasing the concentration of copolymers, the incorporation of pyrene into the micelles resulted in a significant increase in total fluorescence intensity. Thus, the intensity of the third peak in the emission spectra of pyrene increased more than that of the first peak, and the fluorescence intensity ratio of I_3/I_1 increased. The CMC values of the CHS-Mal-DEX and FA-PEG-CHS-Mal-DEX with DS 13.28% and 26.14 % were found to be 2.35, 1.321, 1.05, and 0.613 µg/mL in deionized water, respectively.

SEM and TEM observation

Figure 11A and B exhibit the FE-SEM and TEM images of the optimized formula of Tofa/FA-PEG-CHS-Mal-DEX micelles, which have a uniform spherical shape with a particle size of around 80 nm in SEM and 50 nm in TEM images.

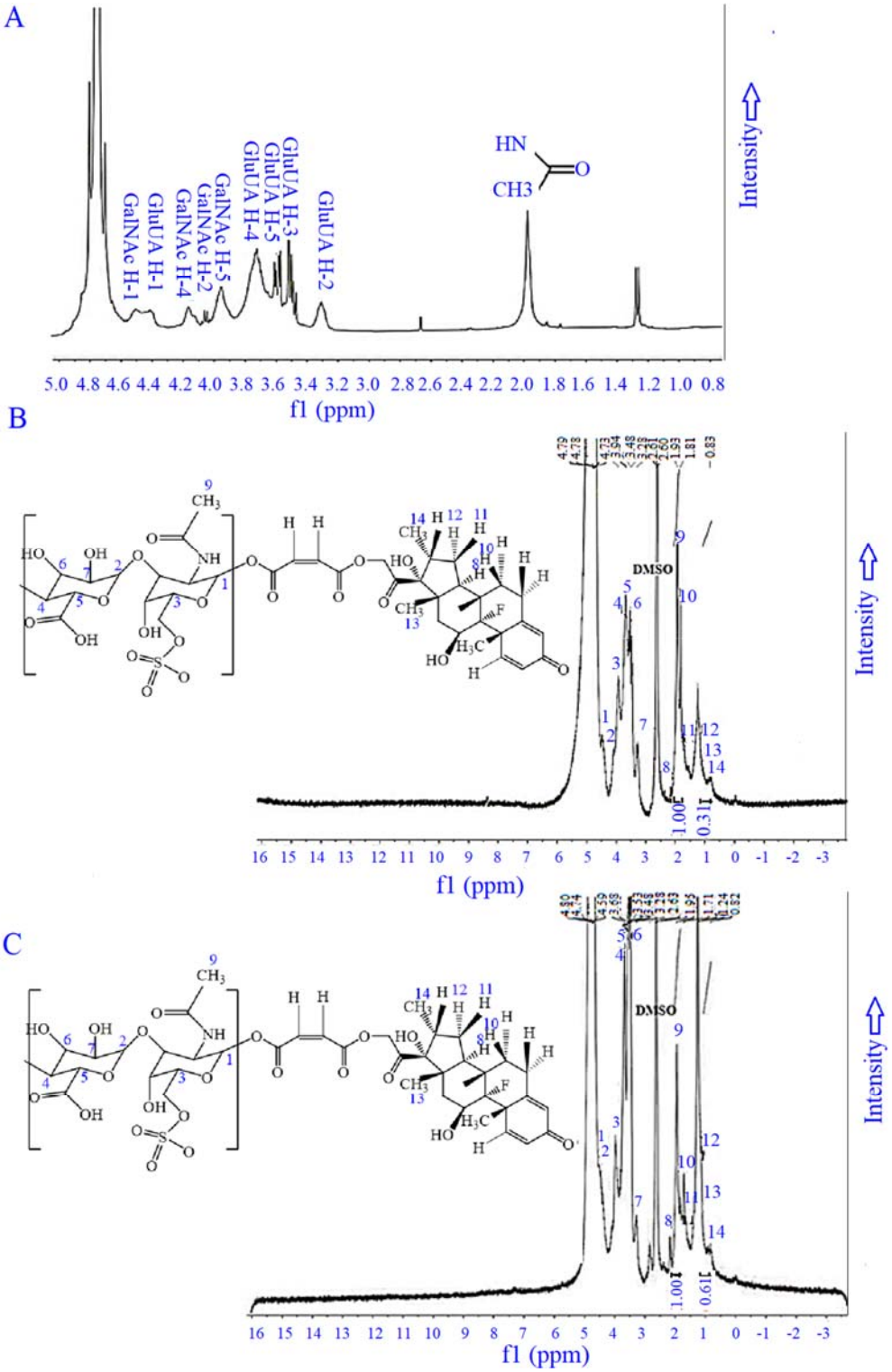

Fig. 7. [1]HNMR spectra of (A) CHS, (B) CHS-Mal-DEX with DS of 10%, and (C) CHS-Mal-DEX with DS of 20%. CHS, Chondroitin sulfate; Mal, maleic; DEX, dexamethasone; DS, degree of substitution.

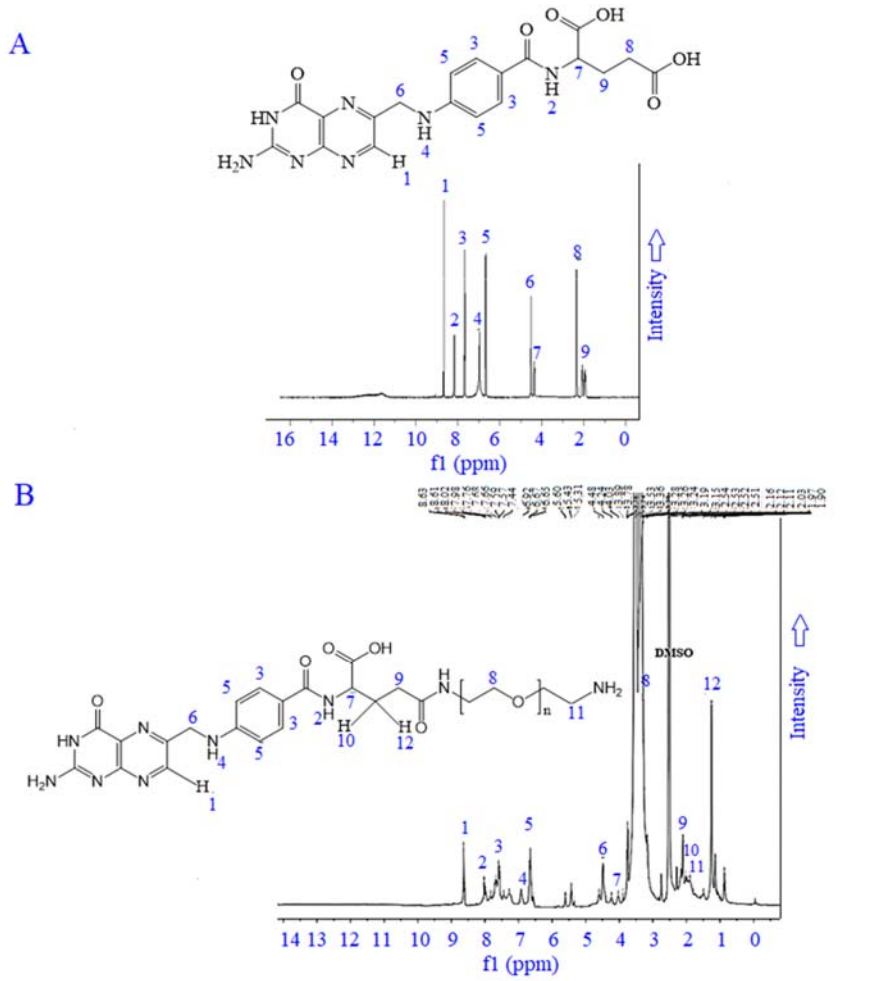

Fig. 8. [1]HNMR spectra of (A) FA and (B) FA-PEG. FA, Folic acid; PEG, polyethylene glycol.

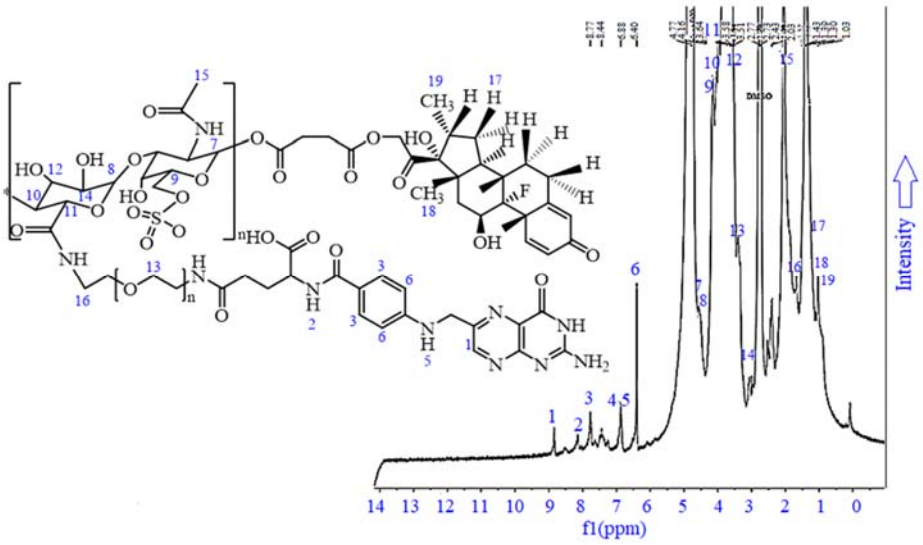

Fig. 9. [1]HNMR spectra of FA-PEG-CHS-Mal-DEX. FA, Folic acid; PEG, polyethylene glycol; CHS, chondroitin sulfate; Mal, maleic; DEX, dexamethasone.

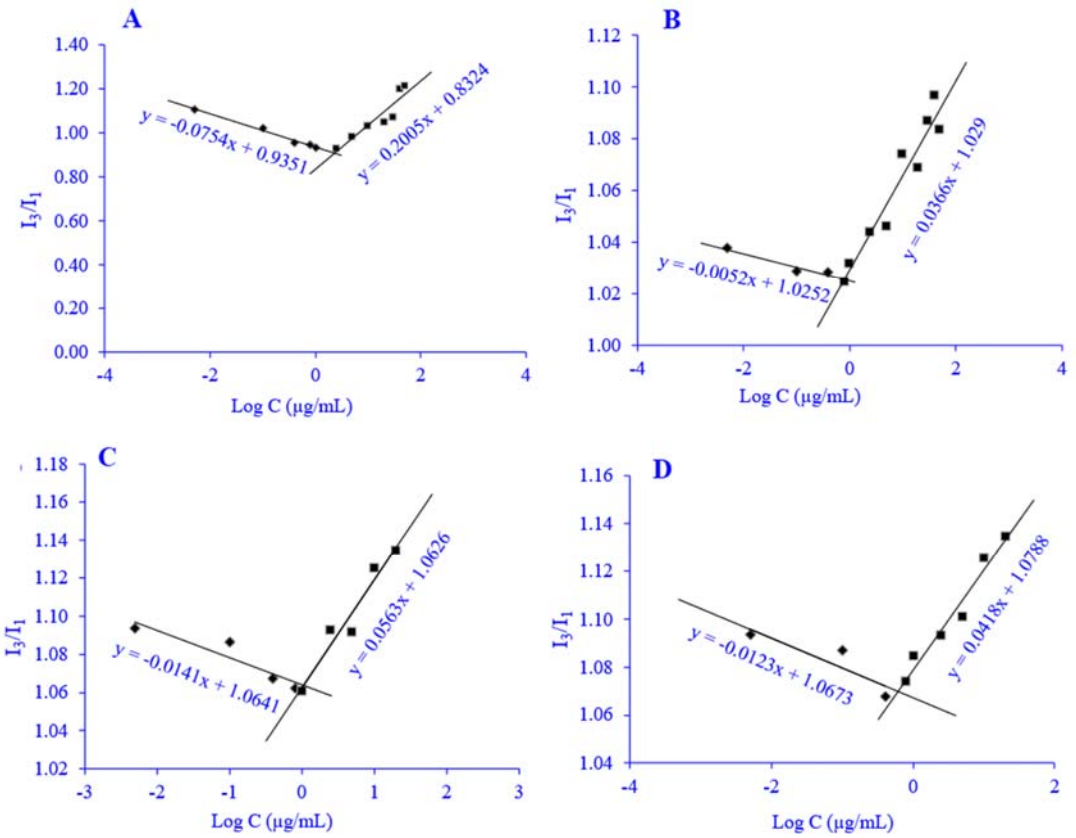

Fig. 10. CMC of (A and B) CHS-Mal-DEX with DS of 10% and 20%; (C and D) FA-PEG-CHS-Mal-DEX with DS of 10% and 20%, respectively. FA, Folic acid; PEG, polyethylene glycol; CHS, chondroitin sulfate; Mal, maleic; DEX, dexamethasone; DS, degree of substitution.

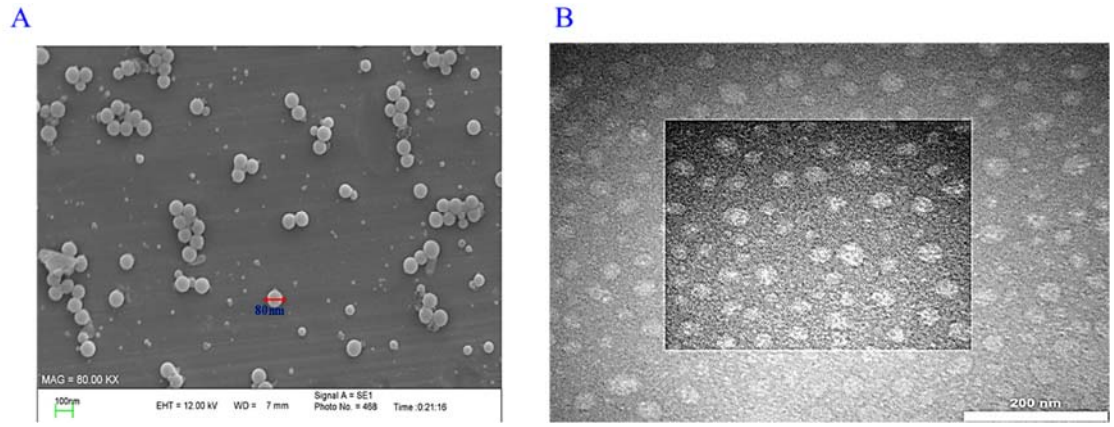

Fig. 11. Morphological evaluation of Tofa/FA-PEG-CHS-Mal-DEX using (A) SEM and (B) TEM observation. Tofa, Tofacitinib; FA, folic acid; PEG, polyethylene glycol; CHS, chondroitin sulfate; Mal, Maleic; DEX, dexamethasone.

Incorporation of Tofa into the micelles

In this study, to obtain the micelles with the most optimal particle size and highest EE, first, Tofa was loaded into the FA-PEG-CHS-Mal-DEX polymeric micelles by two different physical methods, namely dialysis and the probe-type ultrasonication technique at DS 20% (Table 1). Then, the best method was selected and various designs were tested for FA-PEG-CHS-Mal-DEX polymeric micelles to find the optimized formulation of micelle among various DS and D/P ratios.

Table 2 shows the effect of initial drug and incorporation methods on the EE and other physical properties of the micelles. As shown in Table 2, the polymeric micelles' particle sizes ranged from 138 to 390 nm with a PDI of 0.27 to 0.7. As illustrated in Fig. 12A, the DS and D/P ratios' parameters had a significant effect on particle size ($P < 0.05$). Increasing the DS of DEX led to a decrease in the particle size. Decreasing the D/P ratio led to an increase in particle size ($P < 0.05$).

As shown in Table 1, the zeta potential of the micelles obtained from the Probe-type ultrasonication technique became less negative as the initial drug concentration increased. In addition, the EE of the micelles prepared with this technique was not significantly changed by increasing the D/P ratio. All of these results were probably due to the surface interaction of the drug with micelles. So, all of these findings confirm that the dialysis technique is the best method for micelle preparation.

In the present study, the pH-sensitive micelles physically entrapped Tofa, as a hydrophobic drug. As exhibited in Table 2, EE is in the range of 44.11% to 82.63%. As illustrated in Fig. 12B, by increasing the DS ratio, the EE of Tofa in the micelles increased significantly ($P < 0.05$) and the D/P ratio decreased ($P < 0.05$). The third factor affecting EE is solvent types ($P < 0.001$). According to the results, micelles prepared in DMSO had significantly higher EE compared to DMF.

In vitro drug release

As illustrated in Fig. 13 for micelles (FA-PEG-CHS-Mal-DEX polymeric micelles DS 20%, D/P 0.2) obtained from the Probe-type ultrasonication technique due to surface interaction of the drug with micelle and presence of free drug, about 50% of the drug was released in PBS (pH 7.4) during 24 h. However, the micelles obtained from the dialysis method released 35% of Tofa in PBS (pH 7.4) during 96 h.

Table 1. Physical properties of FA-PEG-CHS-Mal-DEX with DS 20% with or without Tofa obtained from different methods. Data are presented as mean ± SD, n = 3.

Micelle preparation method	Formulation	D/P (mg)	PS (nm)	PDI	ZP (mV)	EE (%)
Dialysis	Tofa/FA-PEG-CHS-Mal-DEX	0.2	173.06 ± 2.85	0.27 ± 0.08	-17.10 ± 0.20	72.76 ± 2.01
Probe-type ultrasonication technique	FA-PEG-CHS-Mal-DEX		290.26 ± 8.00	0.35 ± 0.03	-19.70 ± 3.5	-
	Tofa/FA-PEG-CHS-Mal-DEX	0.1	169.56 ± 7.00	0.30 ± 0.10	-16.50 ± 2.10	75.01 ± 2.00
	Tofa/FA-PEG-CHS-Mal-DEX	0.2	243.66 ± 7.50	0.50 ± 0.01	-9.06 ± 5.10	71.50 ± 4.90

FA, Folic acid; PEG, polyethylene glycol; CHS, chondroitin sulfate; Mal, maleic; DEX, dexamethasone; DS, degree of substitution; D/P, drug/polymer; ZP, zeta potential; PS, particle size; PDI, poly dispersity index; EE, entrapment efficiency.

Table 2. Proposed formulations by Design Expert 11 for the evaluation of Tofa/FA-PEG-CHS-Mal-DEX micelles using the full factorial design and physical properties of these micelles. Data are presented as mean ± SD, n = 3.

Run	A: DS (%)	B: D/P	C: Solvent	ZP (mV)	PS (nm)	PDI	EE (%)	LE (%)
1	20	0.1	DMSO	-11.96 ± 0.30	220.06 ± 4.10	0.43 ± 0.03	82.63 ± 1.47	7.46 ± 4.78
2	10	0.2	DMSO	-20.36 ± 2.30	211.33 ± 15.00	0.35 ± 0.05	68.83 ± 0.95	11.4 ± 0.15
3	20	0.1	DMF	-14.44 ± 5.25	250.36 ± 11.53	0.62 ± 0.12	50.42 ± 3.45	4.50 ± 0.30
4	20	0.2	DMF	-18.56 ± 1.33	184.66 ± 8.20	0.63 ± 0.08	44.40 ± 2.20	7.40 ± 0.27
5	10	0.1	DMF	-15.0 ± 2.20	390.01 ± 12.20	0.70 ± 0.15	44.11 ± 5.46	4.11 ± 0.55
6	10	0.2	DMF	-12.0 ± 1.25	330.02 ± 11.28	0.45 ± 0.10	42.13 ± 1.20	7.21 ± 0.20
7	10	0.1	DMSO	-13.0 ± 0.45	365.01 ± 15.00	0.66 ± 0.17	72.71 ± 1.30	6.56 ± 0.20
8	20	0.2	DMSO	-17.10 ± 0.20	173.06 ± 2.85	0.27 ± 0.08	72.76 ± 2.01	12.46 ± 0.6

Tofa, Tofacitinib; FA, folic acid; PEG, polyethylene glycol; CHS, chondroitin sulfate; Mal, maleic; DEX, dexamethasone; DS, degree of substitution; D/P, drug/ polymer; ZP, zeta potential; PS, particle size; PDI, poly dispersity index; EE, entrapment efficiency; LE, loading efficiency.

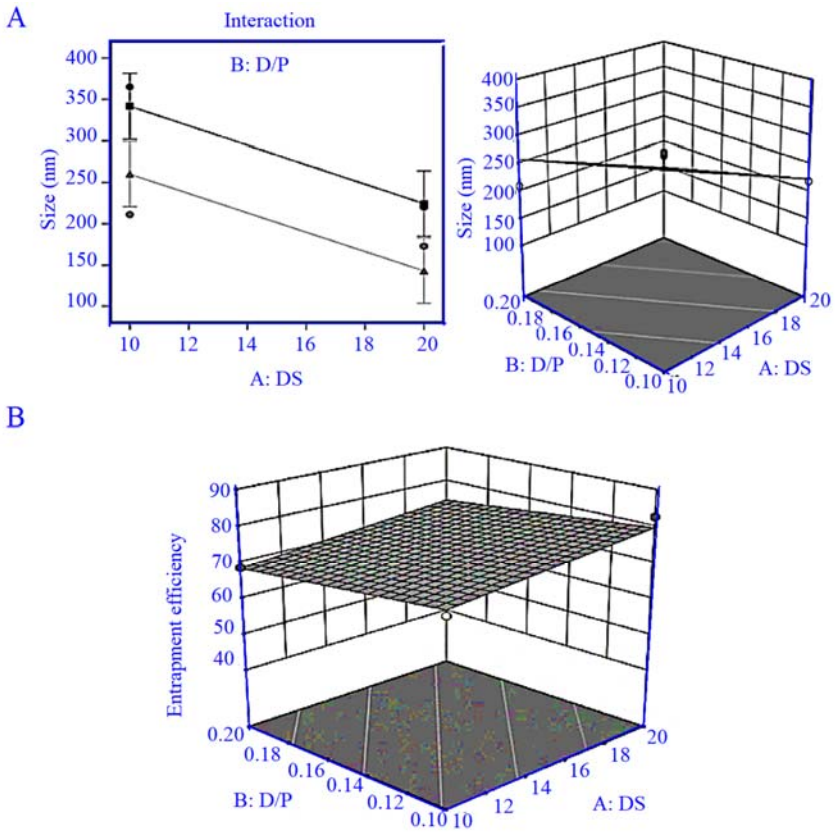

Fig. 12. The effect of D/P ratio and DS on physical properties. (A) particle size and (B) entrapment efficiency. D/P, Drug/polymer; DS, degree of substitution.

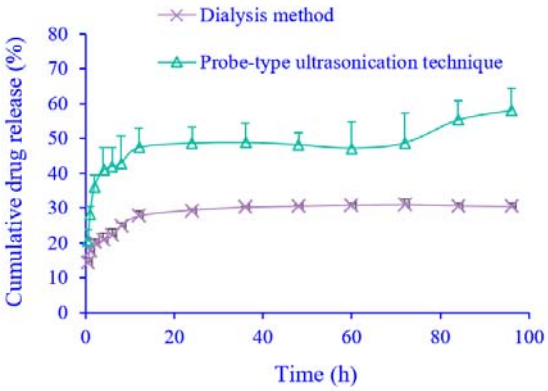

Fig. 13. Cumulative release of tofacitinib in pH 7.4 from micelles that is prepared by dialysis method and probe ultrasonication technique.

In this study, to evaluate the effects of pH on drug release from polymeric micelles, *in vitro* drug release was evaluated under physiological (PBS pH 7.4) and acidic (PB, pH 5) conditions at 37 °C. Figure 14 exhibits cumulative drug release profiles from micelles at physiological (Fig. 14A) and acidic (Fig. 14B) pH within 96 h at 37 °C. Profiles indicate that about 40% of Tofa was released from polymeric micelles over 62 h in physiological pH, whereas in acidic conditions, this value was significantly reduced to just 2 h ($P < 0.001$). Results suggested that Tofa release profiles are affected by the pH of the media. Thus, the Tofa release rate increased as the pH of the medium decreased.

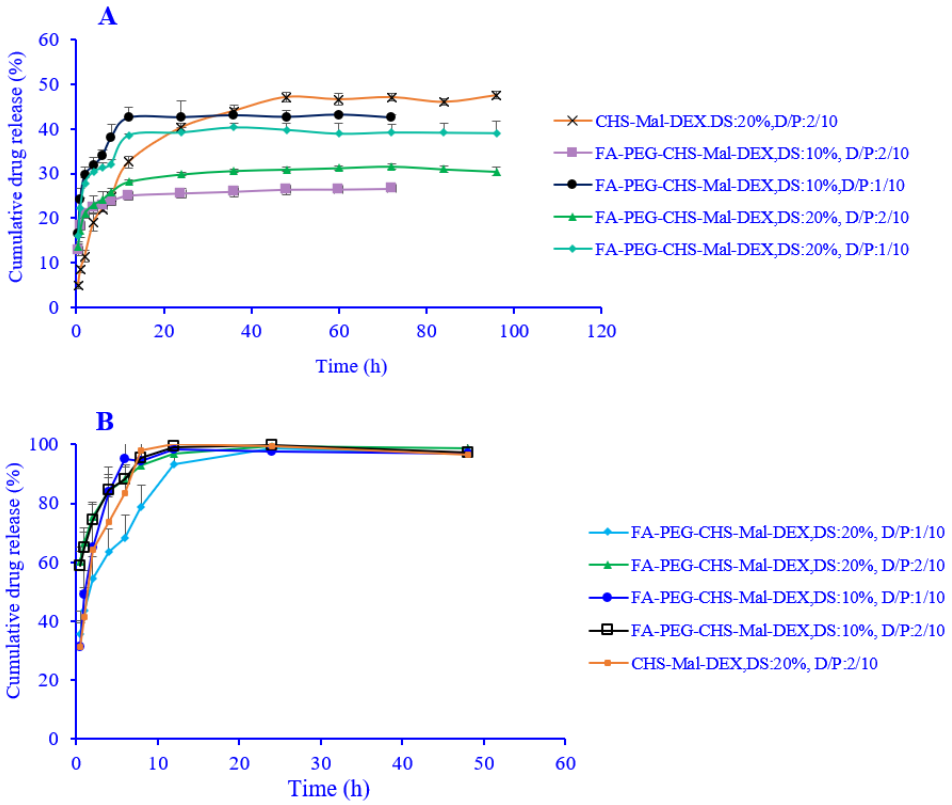

Fig. 14. Cumulative release of tofacitinib in (A) pH 7.4 and (B) pH 5.

Table 3. Predicted and acquired results for the optimal formulation of Tofa/FA-PEG-CHS-Mal-DEX with DS of 20%, D/P of 0.2, and DMSO as the solvent. Data are presented as mean ± SD, n = 3.

Parameters	PS (nm)	ZP (mV)	PDI	EE (%)	LE (%)	Desirability
Predicted values	143.042	-17.52	0.301	74.345	11.795	0.965
Actual values	173.1 ± 2.85	-17.1 ± 0.20	0.272 ± 0.08	72.76 ± 2.01	12.46 ± 0.6	-
Error (%)	20	2.3	9.63	2.13	5.63	-

Tofa, Tofacitinib; FA, folic acid; PEG, polyethylene glycol; CHS, chondroitin sulfate; Mal, maleic; DEX, dexamethasone; DS, degree of substitution; D/P, drug/ polymer; ZP, zeta potential; PS, particle size; PDI, poly dispersity index; EE, entrapment efficiency; LE, loading efficiency.

Table 4. Physical properties of the optimized formula of CHS-Mal-DEX and FA-PEG-CHS-Mal-DEX with DS 20% with or without Tofa. Data are presented as mean ± SD, n = 3.

Formulation	D/P (mg)	PS (nm)	PDI	ZP (mV)	EE (%)
FA-PEG-CHS-Mal-DEX	-	138.7 ± 8.00	0.577 ± 0.138	-18.46 ± 1.76	-
Tofa/FA-PEG-CHS-Mal-DEX	2/10	173.1 ± 2.85	0.272 ± 0.08	-17.10 ± 0.20	72.76 ± 2.01
CHS-Mal-DEX	-	200.2 ± 3.00	0.489 ± 0.045	-29.20 ± 0.62	-
Tofa/CHS-Mal-DEX	2/10	188.0 ± 10.9	0.615 ± 0.060	-20.13 ± 1.42	50.96 ± 2.49

Tofa, Tofacitinib; FA, folic acid; PEG, polyethylene glycol; CHS, chondroitin sulfate; Mal, maleic; DEX, dexamethasone; DS, degree of substitution; D/P, drug/ polymer; ZP, zeta potential; PS, particle size; PDI, poly dispersity index; EE, entrapment efficiency.

Optimization

Based on the smallest particle size and maximum EE, the optimized formula with a desirability factor of 0.965 with variable levels at 20 for DS, 0.2 for D/P, and DMSO as a solvent was selected. Table 3 illustrates the predicted and experimental values of dependent variables as well as the percentage of prediction error. The physical properties of the optimized formula of FA-PEG-CHS-Mal-DEX and CHS-Mal-DEX are exhibited in Table 4.

Stability studies of the micelles

Adsorption of serum proteins to nanoparticles in an *in vivo* situation led to reduced stability. For this purpose, stability studies of micelles in the presence of serum were investigated. As illustrated in Fig. 15, the particle size of the Tofa-loaded FA-PEG-CHS-Mal-DEX micelles did not change significantly after 48 h of incubation in PBS containing 10% FBS at pH 7.4. At the same time, in Tofa/CHS-Mal-DEX, the ratio (t_i/t_0) increased clearly, indicating significant absorption and aggregation of these micelles. According to the results of Table 5, after 2 months of storage, the particle size and PDI of lyophilized FA-PEG-CHS-Mal-DEX and CHS-Mal-DEX polymeric micelles slightly increased, which is a sign of aggregation, but this result may also be the consequence of residual water in the formula. The zeta potential decreased somewhat, indicating stability of micelles during storage. The EE did not change after 2 months of storage.

Viability of the cell culture

For investigation of the toxicity of micelles, the cell viabilities of blank micelles, free Tofa, and Tofa-loaded folate-targeted and non-folate-targeted micelles towards the L929 and RAW 264.7 cell lines were examined by MTT assay. As shown in Fig. 16, the cell viabilities were more than 80% when the cells were incubated with free Tofa at the highest concentration of 10 µg/mL in L929 and 1 µg/mL for RAW 264.7 cells, but blank micelles and Tofa-loaded micelles had no significant cytotoxicity up to 1 and 10 µg/mL of Tofa in RAW 264.7 cells and L929 cell lines, respectively. By increasing the concentration of Tofa in both groups of micelles, the cell viability of L929 increased. This result may be due to the antioxidant and anti-inflammatory effect of CHS in the L929 fibroblastic cell line separately and in combination with Tofa (47).

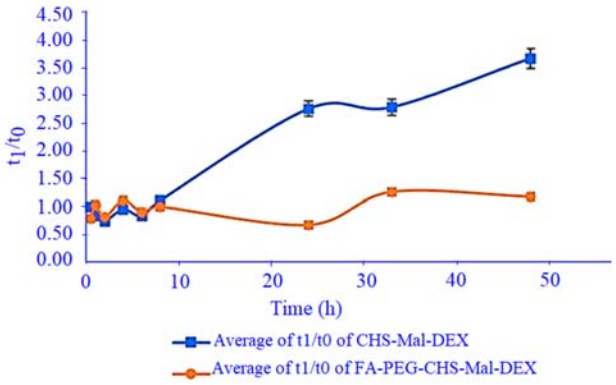

Fig. 15. Particle size change evaluation of Tofa-loaded micelles in PBS containing FBS (10% v/v) at 37 ℃. t_0: the average diameter of micelles in PBS before FBS treatment; t_1: the average diameter of micelles in PBS after FBS treatment over 48h. PBS, Phosphate-buffered solution; FBS, fetal bovine serum; FA, folic acid; PEG, polyethylene glycol; CHS, chondroitin sulfate; Mal, maleic; DEX, dexamethasone.

Table 5. Physical properties of the lyophilized optimal formula of Tofa/CHS-Mal-DEX and Tofa/FA-PEG-CHS-Mal-DEX after storage for 2 months at 4 ℃. Data are presented as mean ± SD, n = 3.

Formulation	PS (nm)		PDI		ZP (mV)		EE (%)	
	Day 0	Day 60	Day 0	Day 60	Day 0	Day 60	Day 0	Day 60
Tofa/FA-PEG-CHS-Mal-DEX	173.± 2.85	231.5 ± 12.70	0.27 ± 0.089	0.39 ± 0.14	-17.10 ± 0.20	-22.16 ± 0.96	72.76 ± 2.01	70.53 ± 1.83
Tofa/CHS-Mal-DEX	188.0 ± 10.9	271.33 ± 14.07	0.61 ± 0.060	0.44 ± 0.026	-20.1± 1.42	-28.5 ± 1.11	50.96 ± 2.49	48.35 ± 1.22

Tofa, Tofacitinib; FA, folic acid; PEG, polyethylene glycol; CHS, chondroitin sulfate; Mal, maleic; DEX, dexamethasone; ZP, zeta potential; PS, particle size; PDI, poly dispersity index; EE, entrapment efficiency.

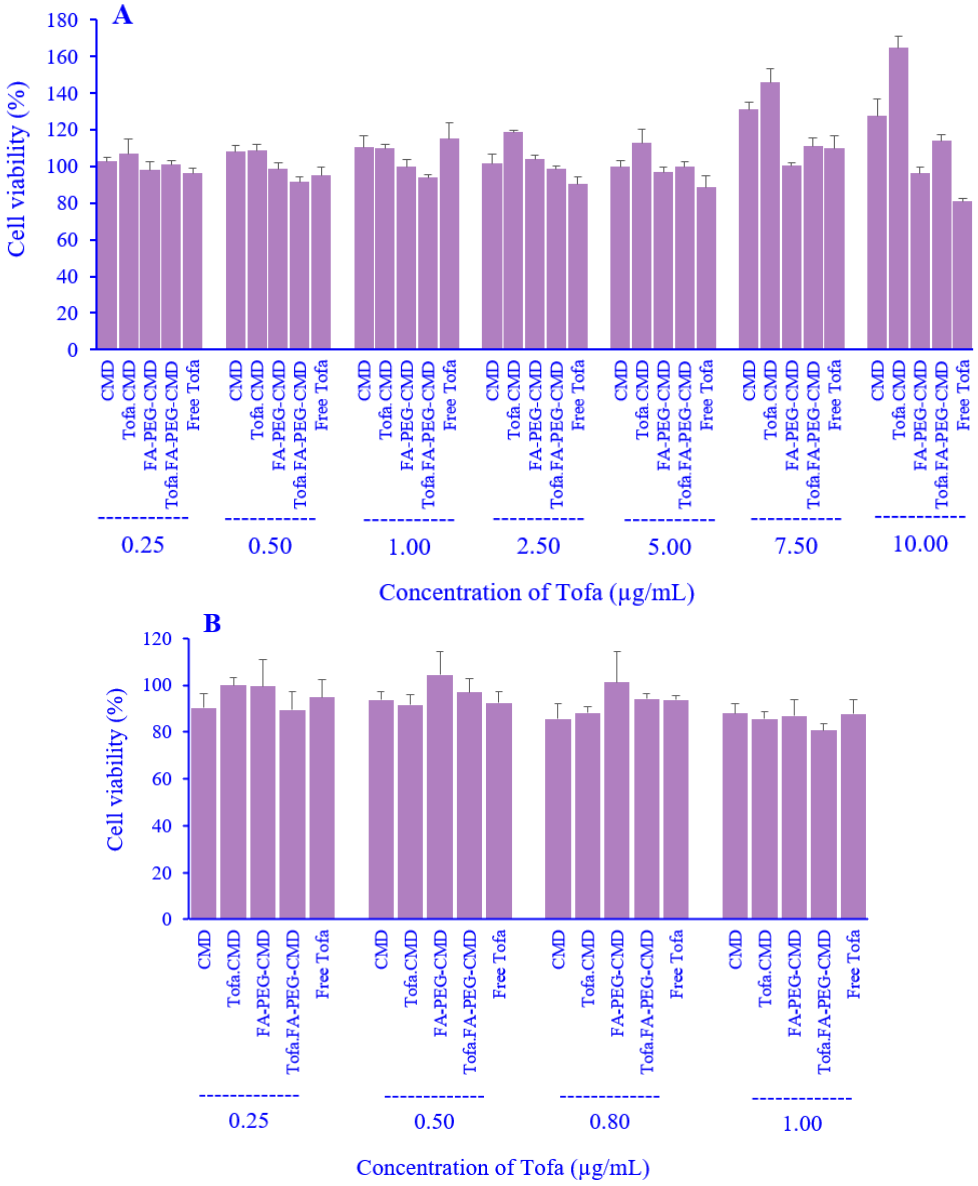

Fig. 16. Effect of different concentrations of CHS-Mal-DEX (CMD, blank micelles), FA-PEG-CHS-Mal-DEX (FA-PEG-CMD), Tofa/CHS-Mal-DEX (Tofa. CMD), Tofa/FA-PEG-CHS-Mal-DEX (Tofa. FA-PEG-CMD), and free drug on the viability of (A) L929 and (B) RAW 264.7 cells. FA, folic acid; PEG, polyethylene glycol; CHS, chondroitin sulfate; Mal, maleic; DEX, dexamethasone; Tofa, tofacitinib.

Cellular uptake studies

Since the CD44 receptor and folate receptor β are overexpressed on activated macrophages in inflammatory tissue, we constructed an inflammatory cell model by activating RAW 264.7 cells. To visualize the effect of each receptor in cellular uptake of macrophage cells, FA-PEG-CHS-Mal-DEX and CHS-Mal-DEX nanoparticles were prepared to target folate receptor β and CD44 receptors, respectively, and CMN instead of Tofa was encapsulated in them. Fluorescent microscopy was used to qualitatively investigate the cellular uptake of free CMN and micelles containing CMN. Figure 17 exhibits the fluorescent microscope images of activated and non-activated RAW 264.7 cells incubated with free CMN and CMN-loaded micelles within 4 and 6 h, two common times for cellular uptake analysis according to the numerous studies (15,16,36). As seen in Fig. 17A, CMN-loaded micelles showed strong fluorescence intensity at each

time point compared to free CMN in activated RAW 264.7 cells. However, the CMN uptake into RAW 264.7 cells without activation was almost invisible (Fig. 17B). That might be due to the non-opsonic phagocytosis of nanoparticles in non-activated macrophages. For activated RAW 264.7 cells, the CMN uptake of FA-PEG-CHS-Mal-DEX was more than CHS-Mal-DEX (Fig. 17A). In addition, the quantitative results of flow cytometer analysis (Fig. 17C) demonstrated that the CMN delivered by FA-PEG-CHS-Mal-DEX (86.4%) was significantly greater than CHS-Mal-DEX (69.3%) and free CMN (49.2%), respectively.

In vitro anti-inflammatory assay in activated macrophages RAW264.7

Free Tofa (0.8 μg/mL), FA-PEG-CHS-Mal-DEX, and CHS-Mal-DEX micelles containing Tofa (0.8 μg/mL) were assayed for their anti-inflammatory responses. As illustrated in Fig. 18A, all treatments could reduce the production of IL-6, but Tofa-loaded micelles significantly reduced IL-6 more than free Tofa. FA-PEG-CHS-Mal-DEX and CHS-Mal-DEX increased the anti-inflammatory efficacy of Tofa because of CD44 and folate receptor targeting. After 24 h, there is no significant difference between Tofa-loaded micelles.

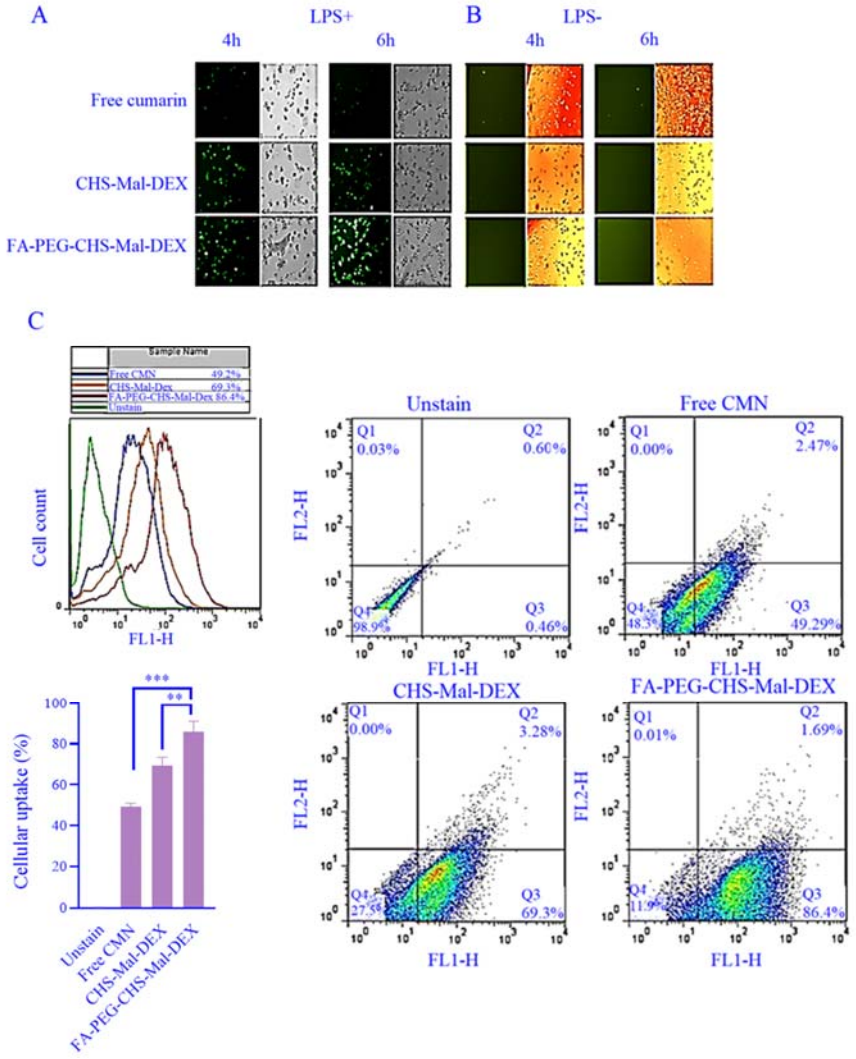

Fig. 17. Intracellular uptake of coumarin-loaded CHS-Mal-DEX and FA-PEG-CHS-Mal-DEX by RAW 264.7 cells activated by (A) LPS (+), (B) nonactivated (−), and (C) intracellular uptake of CMN loaded micelles by flow cytometry. $^{**}P < 0.01$ and $^{***}P < 0.001$ indicate significant differences between designated groups.FA, folic acid; PEG, polyethylene glycol; CHS, chondroitin sulfate; Mal, maleic; DEX, dexamethasone; Tofa, tofacitinib; LPS, lipopolysaccharide; CMN, coumarin.

Folate competitive inhibition assay

The result of the competition cell study exhibited that the IL-6 of cells treated with Tofa-loaded FA-PEG-CHS-Mal-DEX in culture media containing 40 µg/mL FA was significantly higher than the cell supernatant treated with Tofa /FA-PEG-CHS-Mal-DEX in free FA culture media (Fig. 18B). This result confirmed the effect of folate receptor in the internalization of Tofa in activated macrophages.

To investigate the cellular uptake of FA-PEG-CHS-Mal-DEX micelles through the folate receptors, a competitive inhibition test was performed by adding 40 µg/mL free FA in the culture medium to saturate folate receptors on RAW 264.7 activated macrophages. Analysis of fluorescence intensity data from Fig. 17C to Fig. 19 indicates that CMN-loaded FA-PEG-CHS-Mal-DEX micelles exhibited a higher fluorescence intensity (86.1%) compared to the medium containing 40 µg/mL folic acid (73.06%).

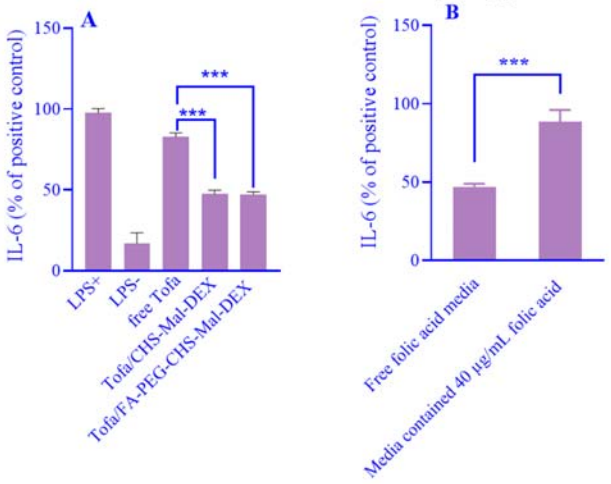

Fig. 18. *In vitro* anti-inflammatory effect of different formulas (A) Tofa/CHS-Mal-DEX and Tofa/FA-PEG-CHS-Mal-DEX in activated macrophages RAW264.7 in free folic acid media and (B) Tofa/FA-PEG-CHS-Mal-DEX in different media. ***$P < 0.001$ indicates significant differences between designated groups. FA, folic acid; PEG, polyethylene glycol; CHS, chondroitin sulfate; Mal, maleic; DEX, dexamethasone; Tofa, tofacitinib.

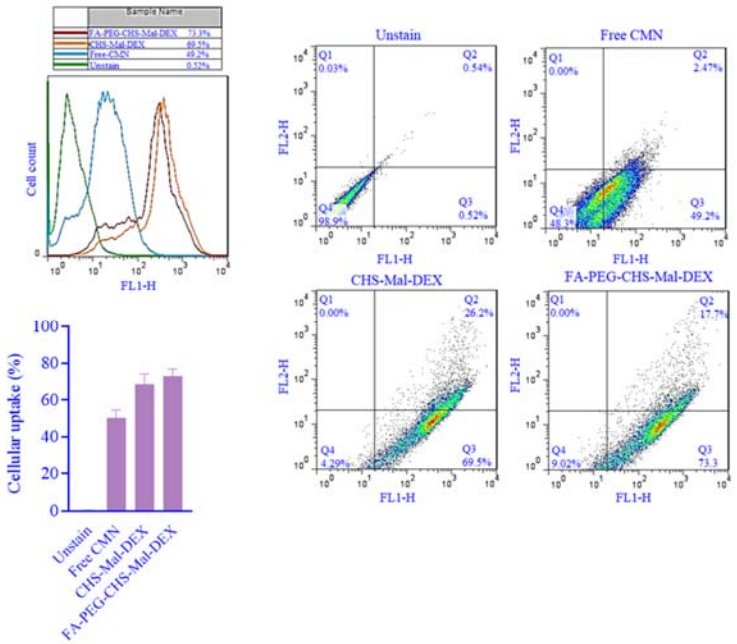

Fig. 19. Intracellular uptake of CMN-loaded FA-PEG-CHS-Mal-DEX by RAW 264.7 cells in the media containing 40 µg/mL free FA. FA, folic acid; PEG, polyethylene glycol; CHS, chondroitin sulfate; Mal, maleic; DEX, dexamethasone.

DISCUSSION

The successful synthesis of the CHS-Mal-DEX and FA-PEG-CHS-Mal-DEX copolymers was confirmed by FT-IR and 1H-NMR spectroscopy.

The CMC values of the copolymers were determined using pyrene as a probe. When the DS of the hydrophobic domain was increased, the CMC values decreased, which may be due to the inner hydrophobic interactions amongst DEX molecules being increased by greater DS. This behavior is consistent with previous studies, which have shown that increasing the hydrophobic domain of amphiphilic copolymers enhances the stability of the micelles and reduces their CMC (29-31).

FE-SEM and TEM analyses confirmed the successful formation of spherical micelles with sizes appropriate for prolonged circulation and reduced immune clearance. While SEM highlighted surface morphology, TEM provided more accurate particle size measurements, consistently showing smaller sizes than DLS due to sample drying effects. The higher resolution of TEM, which involves solvent-suspended samples and minimal agglomeration, offered a clearer view of the internal structure. In contrast, SEM samples, prepared as powders and gold-coated, were more prone to aggregation, explaining the slight size variations observed (48).

In this study, CHS and DEX were conjugated *via* a single pH-sensitive Mal linker, which forms ester bonds with both molecules. This linker undergoes protonation and hydrolysis under acidic pH conditions (approximately 4.5 - 5.5) found in the microenvironment of joint inflammation and within endolysosomes (22-25). Exploring the pH-sensitive nature of Mal and the acidic conditions of inflamed joints and endolysosomes, amphiphilic copolymers, CHS-Mal-DEX and FA-PEG-CHS-Mal-DEX, were designed and synthesized as pH-responsive nanocarriers for drug delivery in RA. These systems aimed to promote targeted intracellular drug release and minimize the systemic side effects of Tofa. Among the physical properties of nanoparticles, particle size has the main effect on the time of blood circulation, therapeutic efficacy, and cellular uptake of nanoparticles in the body. Different studies have confirmed that nanoparticles with sizes below 200 nm can circulate for a long time in the body and escape from reticuloendothelial system clearance (49). This study also highlights the importance of optimizing the D/P ratio and DS of DEX in micelle formation. The physical properties of the micelles, such as their size, charge, and EE, directly influenced the drug loading and release behavior. Increasing the DS of DEX led to a decrease in the particle size because of introducing and enhancing more hydrophobic segments and more hydrophobic interactions in the inner side of the micelles, which led to forming a more condensed core (50,51). Decreasing the D/P ratio led to an increase in particle size. This suggests that the addition of hydrophobic Tofa might induce more compaction of the micellar core (34).

The optimized micelles exhibited high EE values, demonstrating effective drug encapsulation, particularly when the DS ratio increased. This enhancement can be attributed to the stronger hydrophobic interactions within the micelle core, which better encapsulate the hydrophobic Tofa molecule (52).

In terms of formulation methods, the dialysis technique was found to be superior for preparing micelles with higher EE, offering a better balance between stability and drug loading. The choice of solvent was also crucial; micelles prepared in DMSO had significantly higher EE compared to DMF, because of the higher water miscibility of DMSO, leading to rapid micelle formation and entrapping of a greater amount of drug in the micelles (53). These findings are consistent with previous reports on the preparation of folate-targeted, pH-responsive micelles for efficient drug delivery (25).

The *in vitro* drug release experiments highlighted that pH-responsive micelles exhibit a rapid release of Tofa under acidic conditions, mimicking the microenvironment of joint inflammation and the pH of endolysosomes (pH about 4.5 - 5.5) (22). The results suggested that Tofa release profiles are affected by the pH of the media. Thus, the Tofa release rate increased as the pH of the medium decreased. This indicates that the maleic bond is susceptible to

hydrolysis and disassembles the micelles at pH 5. Accelerated drug release in acidic pH from pH-responsive drug delivery systems has previously been reported (54,55).

Compared to other types of stimuli-responsive nanoparticles, such as hydrogen peroxide (H_2O_2)-sensitive polymeric micelles and liposomes (15,56), the pH-sensitive polymeric nanoparticles synthesized in this study demonstrate markedly enhanced physicochemical stability. This improved stability can be attributed to their well-defined polymeric structure, which provides resistance to degradation and environmental stress. For example, after two months of storage in lyophilized form at refrigerated conditions, no significant alterations were observed in key parameters such as particle size, PDI, or drug EE. Moreover, due to the presence of PEG in the structure of the FA-PEG-CHS-Mal-DEX micelles, these nanoparticles are expected to exhibit superior stability in physiological conditions compared to other hydrogen peroxide-sensitive nanoparticles that lack PEG in their structure. So, this optimized formula, Tofa/FA-PEG-CHS-Mal-DEX micelles, because of the inhibition effect of PEG in the adsorption of proteins, has good stability in serum and storage conditions without aggregation.

The cell viability assays revealed that both blank and Tofa-loaded micelles were non-toxic, supporting their biocompatibility for future therapeutic use. Consistent with findings from the current study and others, CHS exhibited anti-inflammatory and antioxidant effects on L929 cells, which represent healthy cells, but not on macrophage cells (47). Notably, increasing the concentration of the nano-micelles enhanced the viability of L929 cells (representing healthy cells) while reducing the viability of macrophage cells. These findings indicate that the synthesized nano-micelles are not toxic to healthy cells but are also beneficial and highly biocompatible with them. The results from the cellular uptake study confirm the pivotal role of the folate receptor and CD44 receptor in enhancing cellular uptake in activated macrophages. The stronger fluorescence and higher uptake observed with FA-PEG-CHS-Mal-DEX micelles suggest that the folate receptor plays a crucial role in facilitating more efficient endocytosis in these cells. Actually, after 6 h, the FA-PEG-CHS-Mal-DEX micelle, because of the high affinity between folic acid and folate receptor, rapid endocytosis, and recycling back to the macrophage surface (57,58), led to more intracellular delivery of coumarin than the CHS-Mal-DEX micelle. The CD44 receptor, because of presenting endocytosis inhibitors affecting the uptake of CHS nanoparticles, has a slow endocytosis process (59,60). According to previous studies, both CD44 and folate receptors were overexpressed in inflammatory conditions and have affinity for intracellular delivery of coumarin in activated macrophages (16,58,61).

Moreover, the anti-inflammatory results emphasize that FA-PEG-CHS-Mal-DEX and CHS-Mal-DEX micelles were more effective at reducing IL-6 production compared to free Tofa, underscoring the enhanced therapeutic potential provided by the receptor-mediated delivery. The comparative study between the two micelle types (FA-PEG-CHS-Mal-DEX and CHS-Mal-DEX) revealed no significant difference in their anti-inflammatory effect after 24 h, because of the overexpression of CD44 and folate receptors on the surface of the macrophage cell line. During a 24-h incubation, all of the nanoparticles, either folate-targeted or non-folate-targeted micelles, entered the cells through CD44 and folate receptors (59,60,62). Although both kinds of micelles have similar anti-inflammatory effects, CHS-Mal-DEX, because of the absence of PEG on its surface, PBS containing 10% FBS, had absorption and aggregation because of the interaction with serum protein. Thus, this micelle may not be suitable for *in vivo* applications. So, the FA-PEG-CHS-Mal-DEX micelle, because of the inhibition effect of PEG in the adsorption of serum proteins, has good stability and this micelle is suitable for *in vitro* and *in vivo* applications.

In the competitive inhibition assay, the elevated IL-6 levels upon the addition of FA further validate the contribution of folate receptors in the cellular uptake of FA-PEG-CHS-Mal-DEX micelles.

Overall, the micellar formulations developed in this study exhibit promising characteristics for the targeted delivery of Tofa, offering a method for reducing side effects. These findings suggest that receptor-targeted micelles, especially those incorporating PEG for stability, offer significant advantages for delivering therapeutic agents in inflammatory conditions like RA. The combination of efficient cellular uptake and enhanced anti-inflammatory activity makes FA-PEG-CHS-Mal-DEX micelles a promising candidate for further development in targeted drug delivery for inflammatory diseases.

CONCLUSION

Tofa-loaded multifunctional micelles were successfully developed using a biocompatible polymer *via* the dialysis method. Comprehensive characterization through FE-SEM, TEM, and DLS confirmed uniform spherical particles with an average size below 200 nm and a stable zeta potential, supporting their suitability for the EPR effect and prolonged systemic circulation. Surface functionalization with folate and CHS significantly improved cellular uptake in activated RAW 264.7 macrophages, leading to a substantial reduction in IL-6 levels compared to free Tofa, thereby demonstrating superior anti-inflammatory activity. Cytotoxicity assays using L929 fibroblasts confirmed excellent biocompatibility of both blank and drug-loaded micelles, with significantly lower toxicity than the free drug. In conclusion, these pH-responsive, folate-targeted micelles present a promising nanoplatform for targeted delivery of Tofa in RA therapy, with the potential to enhance treatment efficacy and reduce systemic side effects through improved targeting and reduced dosing requirements.

Acknowledgments

The content of this paper was extracted from the Ph.D. thesis submitted by Z. Ansarypour, which was financially supported by the Vice Chancellery of Research of Isfahan University of Medical Sciences through Grant No. 399644.

Conflict of interest statements

The authors declared no conflict of interest in this study.

Authors' contributions

Z. Ansarypour carried out the experiments and wrote the manuscript. J. Emami conceived, designed, and supervised the project, reviewed and edited the study protocol, and revised the manuscript. F. Hassanzadeh supervised the synthesis of the copolymer and participated in the management of the study. M. Aghaei supervised the *in vitro* evaluation of the study. M. Minaeiyan reviewed the study protocol. N.M. Davies revised and edited the manuscript. M. Rezazadeh helped in nanoparticle preparation. The finalized article was read and approved by all authors.

REFERENCES

1. Fauci AS, Langford C. Rheumatoid arthritis. harrisons rheumatology. New York, United States: McGraw-Hill Education;2013.
2. Emami J, Kazemi M, Salehi A. *In vitro* and *in vivo* evaluation of two hydroxychloroquine tablet formulations: HPLC assay development. J Chromatogr Sci. 2021;59(1):71-8. DOI: 10.1093/chromsci/bmaa079
3. Feng X, Chen Y. Drug delivery targets and systems for targeted treatment of rheumatoid arthritis. J Drug Target. 2018;26(10):845-857. DOI: 10.1080/1061186X.2018.1433680.
4. Firestein GS, Budd RC, Gabriel SE, McInnes IB, O'Dell JR. Kelley's textbook of Rheumatology E-Book: Elsevier Health Sciences; 2012. pp. 1116-1137.
5. Singh H, Dan A, Kumawat MK, Pawar V, Chauhan DS, Kaushik A, *et al*. Pathophysiology to advanced intra-articular drug delivery strategies: Unravelling rheumatoid arthritis. Biomaterials. 2023;303:122390. DOI: 10.1016/j.biomaterials.2023.122390
6. Strand V, Kremer J, Wallenstein G, Kanik KS, Connell C, Gruben D, *et al*. Effects of tofacitinib monotherapy on patient-reported outcomes in a randomized phase 3 study of patients with active rheumatoid arthritis and inadequate responses to DMARDs. Arthritis Res Ther. 2015; 17:307,1-12. DOI: 10.1186/s13075-015-0825-9.
7. Wallenstein GV, Kanik KS, Wilkinson B, Cohen S, Cutolo M, Fleischmann R, *et al*. Effects of the oral Janus kinase inhibitor tofacitinib on patient-reported outcomes in patients with active rheumatoid arthritis: results of two Phase 2 randomised controlled trials. Clin Exp Rheumatol. 2016;34(3):430-442. PMID: 27156561.

8. Yu RH, Li X, DuBois D, Almon R, Cao Y, Jusko W. Interactions of tofacitinib and dexamethasone on lymphocyte proliferation. Pharm Res. 2020;37(6):105,1-9. DOI: 10.1007/s11095-020-02827-7.
9. Yu R, Song D, DuBois DC, Almon RR, Jusko WJ. Modeling combined anti-inflammatory effects of dexamethasone and tofacitinib in arthritic rats. AAPS J. 2019;21(5):93,1-19. DOI: 10.1208/s12248-019-0362-6.
10. Nasra S, Bhatia D, Kumar A. Recent advances in nanoparticle-based drug delivery systems for rheumatoid arthritis treatment. Nanoscale Adv. 2022;4(17):3479-3494. DOI: 10.1039/d2na00229a.
11. Siddiqui B, Ur Rehman A, Gul R, Chaudhery I, Shah KU, Ahmed N. Folate decorated chitosan-chondroitin sulfate nanoparticles loaded hydrogel for targeting macrophages against rheumatoid arthritis. Carbohydr Polym. 2024;327:121683. DOI: 10.1016/j.carbpol.2023.121683.
12. Yuan F, Quan LD, Cui L, Goldring SR, Wang D. Development of macromolecular prodrug for rheumatoid arthritis. Adv Drug Deliv Rev. 2012;64(12):1205-1219. DOI: 10.1016/j.addr.2012.03.006.
13. Emami J, Ansarypour Z. Receptor targeting drug delivery strategies and prospects in the treatment of rheumatoid arthritis. Res Pharm Sci. 2019;14(6):471-487. DOI: 10.4103/1735-5362.272534.
14. Ahn J, Miura Y, Yamada N, Chida T, Liu X, Kim A, *et al*. Antibody fragment-conjugated polymeric micelles incorporating platinum drugs for targeted therapy of pancreatic cancer. Biomaterials. 2015;39:23-30. DOI: 10.1016/j.biomaterials.2014.10.069.
15. Wang Z, Zhan C, Zeng F, Wu S. A biopolymer-based and inflammation-responsive nanodrug for rheumatoid arthritis treatment via inhibiting JAK-STAT and JNK signalling pathways. Nanoscale. 2020;12(45):23013-23027.
16. Zhang N, Xu C, Li N, Zhang S, Fu L, Chu X, *et al*. Folate receptor-targeted mixed polysialic acid micelles for combating rheumatoid arthritis: *in vitro* and *in vivo* evaluation. Drug Deliv. 2018;25(1):1182-1191. DOI: 10.1080/10717544.2018.1472677.
17. Naor D, Nedvetzki S. CD44 in rheumatoid arthritis. Arthritis Res Ther. 2003;5(3):105-115. DOI: 10.1186/ar746.
18. Gorantla S, Gorantla G, Saha RN, Singhvi G. CD44 receptor-targeted novel drug delivery strategies for rheumatoid arthritis therapy. Expert Opin Drug Deliv. 2021;18(11):1553-1557. DOI: 10.1080/17425247.2021.1950686.
19. Ruffell B. Regulation and function of hyaluronan binding by CD44 in the immune system. University of British Columbia; 2008. Retrieved from https://open.library.ubc.ca/collections/ubctheses/24/items/1.0066510.
20. Van Der Heijden JW, Oerlemans R, Dijkmans BA, Qi H, Laken CJVD, Lems WF, *et al*. Folate receptor β as a potential delivery route for novel folate antagonists to macrophages in the synovial tissue of rheumatoid arthritis patients. Arthritis Rheum. 2009;60(1):12-21. DOI: 10.1002/art.24219.
21. Chandrupatla DM, Molthoff CF, Lammertsma AA, van der Laken CJ, Jansen G. The folate receptor β as a macrophage-mediated imaging and therapeutic target in rheumatoid arthritis. Drug Deliv Transl Res. 2019;9:366-378. DOI: 10.1007/s13346-018-0589-2.
22. Wang X, Cao W, Sun C, Wang Y, Wang M, Wu J. Development of pH-sensitive dextran-based methotrexate nanodrug for rheumatoid arthritis therapy through inhibition of JAK-STAT pathways. Int J Pharm. 2022;622:121874,1-12. DOI: 10.1016/j.ijpharm.2022.121874.
23. Sauvage E, Amos D, Antalek B, Schroeder K, Tan J, Plucktaveesak N, *et al*. Amphiphilic maleic acid-containing alternating copolymers—1. Dissociation behavior and compositions. J Polym Sci Part B Polym. Phys. 2004;42(19):3571-3583. DOI:10.1002/polb.20202.
24. Popescu I, Prisacaru I, Suflet D, Fundueanu G. Thermo- and pH-sensitivity of poly (N-vinylcaprolactam-co-maleic acid) in aqueous solution. Polym Bull. (Berl.). 2014;71:2863-2880. DOI:10.1007/s00289-014-1227-x.
25. Baniak B. Maleic acid amide derivatives as pH-sensitive linkers for therapeutic peptide conjugation. 2023 Available at: https://studenttheses.uu.nl/handle/20.500.12932/45622.
26. Barry E, Borer LL. Experiments with aspirin. J Chem Educ. 2000;77(3):354-355. DOI: 10.1021/ed077p354.
27. Emami J, Kazemi M, Hasanzadeh F, Minaiyan M, Mirian M, Lavasanifar A. Novel pH-triggered biocompatible polymeric micelles based on heparin–α-tocopherol conjugate for intracellular delivery of docetaxel in breast cancer. Pharm Dev Technol. 2020;25(4):492-509. DOI: 10.1080/10837450.2019.1711395.
28. Emami J, Rezazadeh M, Hasanzadeh F, Sadeghi H, Mostafavi A, Minaiyan M, *et al*. Development and *in vitro*/*in vivo* evaluation of a novel targeted polymeric micelle for delivery of paclitaxel. Int J Biol Macromol. 2015;80:29-40. DOI: 10.1016/j.ijbiomac.2015.05.062.
29. Kazemi M, Emami J, Hasanzadeh F, Minaiyan M, Mirian M, Lavasanifar A. Pegylated multifunctional pH-responsive targeted polymeric micelles for ovarian cancer therapy:synthesis, characterization and pharmacokinetic study. Int J Polym. Biomater. 2021;70(14):1012-1026. DOI: 10.1080/00914037.2020.1776282.
30. Huang X, Liao W, Zhang G, Kang S, Zhang CY. pH-sensitive micelles self-assembled from polymer brush (PAE-g-cholesterol)-b-PEG-b-(PAE-g-cholesterol) for anticancer drug delivery and controlled release. Int J Nanomedicine. 2017;12:2215-2226. DOI: 10.2147/IJN.S130037.

31. Zhang H, Xu J, Xing L, Ji J, Yu A, Zhai G. Self-assembled micelles based on Chondroitin sulfate/poly (d, l-lactideco-glycolide) block copolymers for doxorubicin delivery. J Colloid Interface Sci. 2017;492:101-111. DOI: 10.1016/j.jcis.2016.12.046.
32. Amjad MW, Amin MCIM, Katas H, Butt AM. Doxorubicin-loaded cholic acid-polyethyleneimine micelles for targeted delivery of antitumor drugs: synthesis, characterization, and evaluation of their *in vitro* cytotoxicity. Nanoscale Res Lett. 2012;7(1):1-9. DOI: 10.1186/1556-276X-7-687.
33. Jafari A, Yan L, Mohamed MA, Wu Y, Cheng C. Well-defined diblock poly (ethylene glycol)-b-poly (ε-caprolactone)-based polymer-drug conjugate micelles for pH-responsive delivery of doxorubicin. Materials. 2020;13(7):1510,1-14. DOI: 10.3390/ma13071510.
34. Liu Y, Sun J, Cao W, Yang J, Lian H, Li X, *et al*. Dual targeting folate-conjugated hyaluronic acid polymeric micelles for paclitaxel delivery. Int J Pharm. 2011;421(1):160-169. DOI: 10.1016/j.ijpharm.2011.09.006.
35. Rangasami VK, Samanta S, Parihar VS, Asawa K, Zhu K, Varghese OP, *et al*. Harnessing hyaluronic acid-based nanoparticles for combination therapy:A novel approach for suppressing systemic inflammation and to promote antitumor macrophage polarization. Carbohydr Polym. 2021;254:117291,1-9. DOI: 10.1016/j.carbpol.2020.117291.
36. Vakilzadeh H, Varshosaz J, Dinari M, Mirian M, Hajhashemi V, Shamaeizadeh N, *et al*. Smart redox-sensitive micelles based on chitosan for dasatinib delivery in suppressing inflammatory diseases. Int J Biol Macromol. 2023;229:696-712. DOI: 10.1016/j.ijbiomac.2022.12.111.
37. Mahmoudzadeh M, Fassihi A, Dorkoosh F, Heshmatnejad R, Mahnam K, Sabzyan H, *et al*. Elucidation of molecular mechanisms behind the self-assembly behavior of chitosan amphiphilic derivatives through experiment and molecular modeling. Pharm Res. 2015;32(12):3899-3915. DOI: 10.1007/s11095-015-1750-y.
38. Pavia DL, Lampman GM, Kriz GS, Vyvyan JR. Introduction to spectroscopy. 2015. Available at: https://www.hdki.hr/_download/repository/Pavia-Introduction-to-Spectroscopy%5B1%5D.pdf.
39. Sun D, Ding J, Xiao C, Chen J, Zhuang X, Chen X. Preclinical evaluation of antitumor activity of acid-sensitive PEGylated doxorubicin. ACS Appl Mater Interfaces. 2014;6(23):21202-21214. DOI: 10.1021/am506178c.
40. Foot M, Mulholland M. Classification of chondroitin sulfate A, chondroitin sulfate C, glucosamine hydrochloride and glucosamine 6 sulfate using chemometric techniques. J Pharm Biomed Anal. 2005;38(3):397-407. DOI: 10.1016/j.jpba.2005.01.026.
41. Suhail M, Chiu IH, Hung MC, Vu QL, Lin IL, Wu PC. *In vitro* evaluation of smart and pH-sensitive chondroitin sulfate/sodium polystyrene sulfonate hydrogels for controlled drug delivery. Gels. 2022;8(7):406,1-18. DOI: 10.3390/gels8070406.
42. Durairaju P, Umarani C, Rajabather JR, Alanazi AM, Periyasami G, Wilson LD. Synthesis and characterization of pyridine-grafted copolymers of acrylic acid–styrene derivatives for antimicrobial and fluorescence applications. Micromachines. 2021;12(6):672,1-17. DOI: 10.3390/mi12060672.
43. Li NN, Lin J, Gao D, Zhang LM. A macromolecular prodrug strategy for combinatorial drug delivery. J Colloid Interface Sci. 2014;417:301-309. DOI: 10.1016/j.jcis.2013.11.061.
44. Duan ZH, Cheng CY, Hai Y, Wang JL. Determination and identification of chondroitin sulfate from tilapia byproducts. Adv Mater Res. 2013;690:1318-1321. DOI: 10.4028/www.scientific.net/AMR.690-693.1318.
45. Sarwar S, Abdul Qadir M, Alharthy RD, Ahmed M, Ahmad S, Vanmeert M, *et al*. Folate conjugated polyethylene glycol probe for tumor-targeted drug delivery of 5-fluorouracil. Molecules. 2022;27(6):1780,1-16. DOI: 10.3390/molecules27061780.
46. Emami J, Kazemi M, Mirian M. Synthesis and in vitro evaluation of self-assembling biocompatible heparin-based targeting polymeric micelles for delivery of doxorubicin to leukemic cells. Res Pharm Sci. 2025;20(1):142-164. DOI: 10.4103/RPS.RPS_197_24.
47. Craciunescu O, Moldovan L, Moisei M, Trif M. Liposomal formulation of chondroitin sulfate enhances its antioxidant and anti-inflammatory potential in L929 fibroblast cell line. J Liposome Res. 2013;23(2):145-153. DOI: 10.3109/08982104.2013.770016.
48. Habibi-Yangjeh A. Re: Why is particle size measured with SEM is bigger than TEM? Retrieved from: 2021. Available at: https://www.researchgate.net/post/Why_is_particle_size_measured_with_SEM_is_bigger_than_TEM2/6041e52986e9b1148a06b243/citation/download
49. Varshosaz J, Taymouri S, Hassanzadeh F, Haghjooy Javanmard S, Rostami M. Folated synperonic-cholesteryl hemisuccinate polymeric micelles for the targeted delivery of docetaxel in melanoma. Biomed Res Int. 2015;2015(1):746093,1-17. DOI: 10.1155/2015/746093.
50. Guo H, Zhang D, Li C, Jia L, Liu G, Hao L, *et al*. Self-assembled nanoparticles based on galactosylated O-carboxymethyl chitosan-graft-stearic acid conjugates for delivery of doxorubicin. Int J Pharm. 2013;458(1):31-38. DOI: 10.1016/j.ijpharm.2013.10.020.
51. Yang X, Cai X, Yu A, Xi Y, Zhai G. Redox-sensitive self-assembled nanoparticles based on alpha-tocopherol succinate-modified heparin for intracellular delivery of paclitaxel. J Colloid Interface Sci. 2017;496:3113-26. DOI: 10.1016/j.jcis.2017.02.033.

52. Li L, Huh KM, Lee YK, Kim SY. Biofunctional self-assembled nanoparticles of folate–PEG–heparin/PBLA copolymers for targeted delivery of doxorubicin. J. Mater Chem. 2011;21(39): 15288-15297.
DOI: 10.1039/C1JM11944C.
53. Opanasopit P, Ngawhirunpat T, Chaidedgumjorn A, Rojanarata T, Apirakaramwong A, Phongying S, *et al*. Incorporation of camptothecin into N-phthaloyl chitosan-g-mPEG self-assembly micellar system. Eur J Pharm Biopharm. 2006;64(3):269-276.
DOI: 10.1016/j.ejpb.2006.06.001.
54. Qiu L, Zhu M, Gong K, Peng H, Ge L, Zhao L, *et al*. pH-triggered degradable polymeric micelles for targeted anti-tumor drug delivery. Mater Sci Eng C Mater Biol Appl. 2017;78:912-922.
DOI: 10.1016/j.msec.2017.04.137.
55. Yan K, Feng Y, Gao K, Shi X, Zhao X. Fabrication of hyaluronic acid-based micelles with glutathione-responsiveness for targeted anticancer drug delivery. J Colloid Interface Sci. 2022;606(Pt 2):1586-1596.
DOI: 10.1016/j.jcis.2021.08.129.
56. Shen Q, Shu H, Xu X, Shu G, Du Y, Ying X. Tofacitinib citrate-based liposomes for effective treatment of rheumatoid arthritis. Pharmazie. 2020;75(4):131-135.
DOI: 10.1691/ph.2020.9154.
57. Varghese B, Vlashi E, Low PS. Folate receptor saturation, recycling, and release kinetics in activated macrophages. Blood. 2008;112(11):4655.
DOI: 10.1182/blood.V112.11.4655.4655.
58. Vichare R, Crelli C, Liu L, McCallin R, Cowan A, Stratimirovic S, *et al*. Folate-conjugated near-infrared fluorescent perfluorocarbon nanoemulsions as theranostics for activated macrophage COX-2 inhibition. Sci Rep. 2023;13:15229,1-17.
DOI: 10.1038/s41598-023-41959-9.
59. Almalik A, Karimi S, Ouasti S, Donno R, Wandrey C, Day PJ, *et al*. Hyaluronic acid (HA) presentation as a tool to modulate and control the receptor-mediated uptake of HA-coated nanoparticles. Biomaterials. 2013;34(21):5369-5380.
DOI: 10.1016/j.biomaterials.2013.03.065.
60. Rios De la Rosa JM, Tirella A, Gennari A, Stratford IJ, Tirelli N. The CD44-mediated uptake of hyaluronic acid-based carriers in macrophages. Adv Healthc Mater. 2017;6(4):1-11.
DOI: 10.1002/adhm.201601012.
61. Zhao J, Zhang X, Sun X, Zhao M, Yu C, Lee RJ, *et al*. Dual-functional lipid polymeric hybrid pH-responsive nanoparticles decorated with cell penetrating peptide and folate for therapy against rheumatoid arthritis. Eur J Pharm Biopharm. 2018;130:39-47.
DOI: 10.1016/j.ejpb.2018.06.020.
62. Tatode A, Agrawal PR, Taksande J, Qutub M, Premchandani T, Umekar M, *et al*. Role of folate receptor and CD44 in targeting of docetaxel and paclitaxel fabricated conjugates for efficient cancer therapy. J Med Surg Public Health. 2025; 100163,1-14.
DOI: 10.1016/j.glmedi.2024.100163.